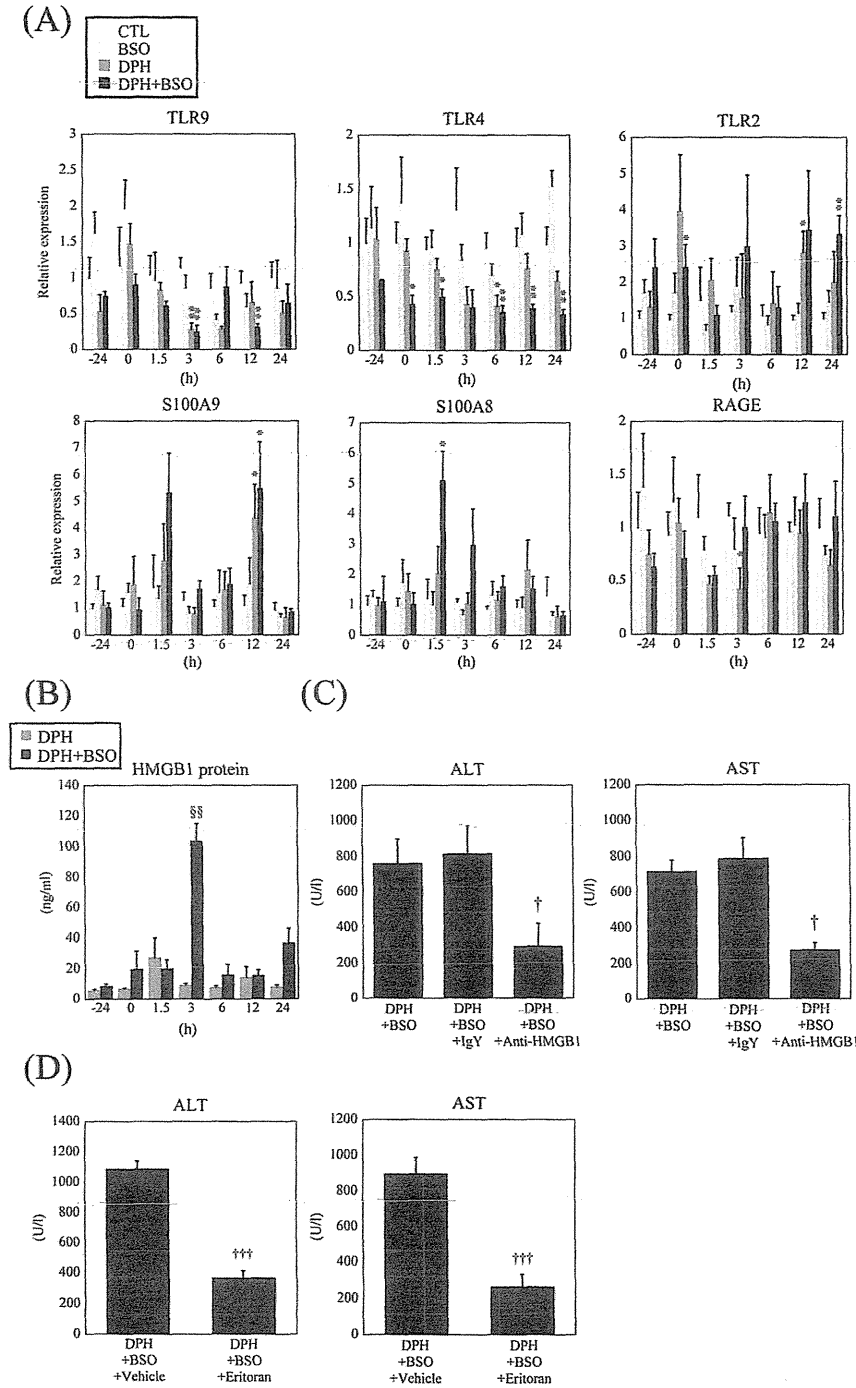

FIG. 4. Time-dependent changes in the hepatic mRNA expression levels of DAMP-related genes and plasma HMGB1 protein levels and the results of the neutralization studies in DPH-induced liver injury. A and B, Mice were IP given DPH at 50 mg/kg for 2 days, followed by oral administration of 100 mg/kg of DPH on days 3 through 5. BSO was IP injected 1 h prior to each DPH administration. Each vehicle was used as a control. At 24 h before (−24) and 0, 1.5, 3, 6, 12, and 24 h after the final DPH treatment, liver and plasma samples were collected to measure the expression of both the hepatic mRNAs of DAMP-related genes and the plasma HMGB1 protein. The expression levels of hepatic mRNAs were normalized to that of Gapdh. C, The effect of an anti-HMGB1 antibody. Mice were IV administered the anti-mouse HMGB1 antibody (200 μg anti-HMGB1 antibody in 0.2 ml sterile PBS) simultaneously with the final DPH treatment. Blood was collected 24 h after the final DPH treatment. D, The effect of eritoran, a TLR4 antagonist, on DPH-induced liver injury. Mice were IV given eritoran (50 μg/mouse in 0.2 ml sterile saline) simultaneously with the final DPH treatment. Blood was collected 24 h after the final DPH treatment. The data are shown as the mean ± SEM. The results of the time-dependent study are taken from 3 to 5 mice, and the other data are taken from 4 to 5 mice. The differences relative to the control mice were considered significant at $*p < .05$, $**p < .01$, compared with the −24 h mice were considered significant at $§§p < .01$ in ELISA, and compared with isotype IgY or vehicle-treated mice were considered significant at $†p < .05$ and $†††p < .001$ in neutralization or antagonist studies, respectively. Abbreviations: BSO, L-buthionine-S,R-sulfoximine; DAMP, damage-associated molecular patterns; DPH, 5,5-diphenylhydantoin; HMGB1, high-mobility group box 1; mRNA, messenger RNA; RAGE, receptor for advanced glycation end products; TLR, toll-like receptor.

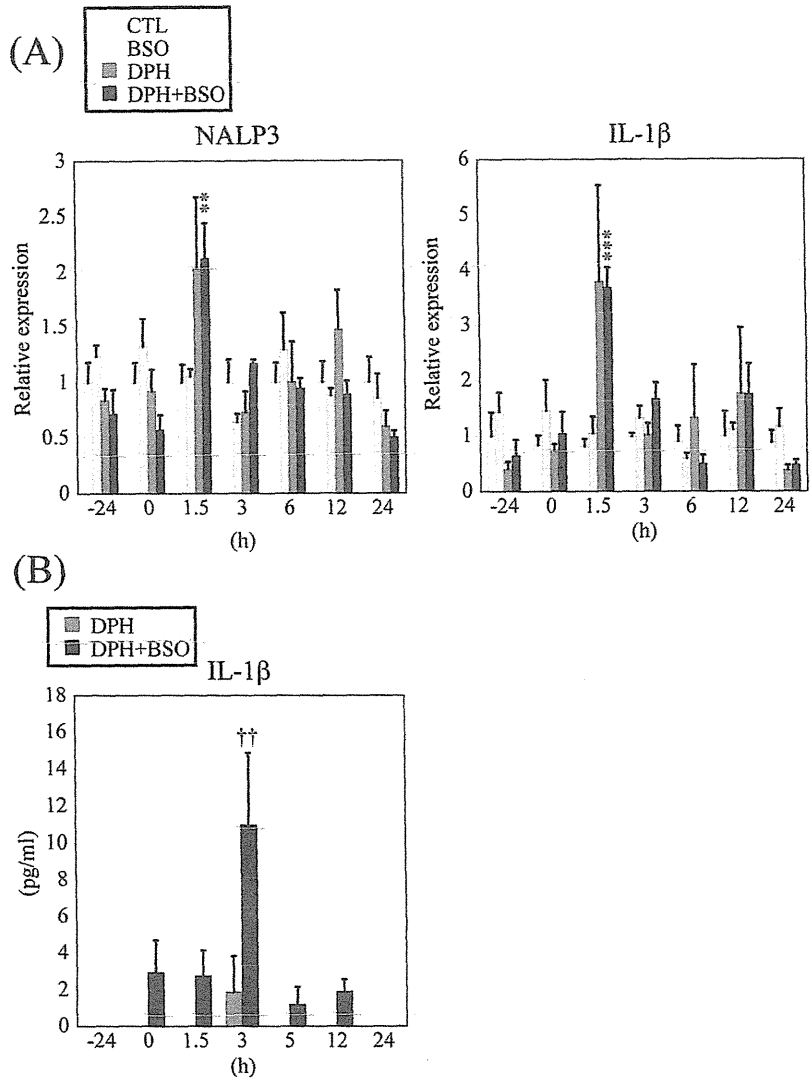

FIG. 5. Time-dependent changes in the hepatic mRNA expression levels of NALP3 and IL-1β (A) and plasma IL-1β protein levels (B) in DPH-induced liver injury. The experimental conditions for DPH treatments and blood and liver collection were the same as those in Figure 4. The data are shown as the mean ± SEM of the results from 3 to 5 mice. The differences relative to the control mice were considered significant at $^{**}p < 0.01$ and $^{***}p < 0.001$, and the -24 h mice were considered significant at $^{\dagger\dagger}p < 0.01$ in ELISA. Abbreviations: DPH, 5,5-diphenylhydantoin; IL, interleukin; NALP3, NACHT-, LRR-, and pyrin domain-containing protein 3; mRNA, messenger RNA.

changes in the hepatic mRNA expression levels of transcription factors for the Th lineage, cytokines, and chemokines (Fig. 6A). The hepatic mRNA expression levels of the Th17 cell-related factors IL-23 p19, IL-6, and ROR-γt were significantly increased at some time points of measurement in mice treated with both DPH and BSO compared with the vehicle-treated mice. However, the expression levels of T-bet, GATA-3, and Foxp3, corresponding to Th1-, Th2-, and regulatory T cell-related factors, respectively, were significantly decreased in mice treated with both DPH and BSO compared with vehicle-treated mice. Following the last administration of DPH in DPH plus BSO-treated mice, the expression levels of chemokines such as MCP-1 and MIP-2 showed a time-dependent increase. The expression levels of MIP-2 were significantly increased at 6–24 h after the last DPH administration in DPH plus BSO-treated mice compared with vehicle-treated mice. However, their levels in the mice given only BSO were not significantly altered compared with those in the mice given the vehicle. These results suggest that Th17 cell-mediated inflammation is involved in DPH-induced liver injury.

We next measured the plasma concentration of the IL-17 protein using an ELISA. A significant increase in concentration was observed at 6 h after the final DPH treatment in the mice given both DPH and BSO, whereas no significant increase was observed in the mice given only DPH (Fig. 6B). To investigate whether IL-17 was involved in DPH-induced liver injury, we

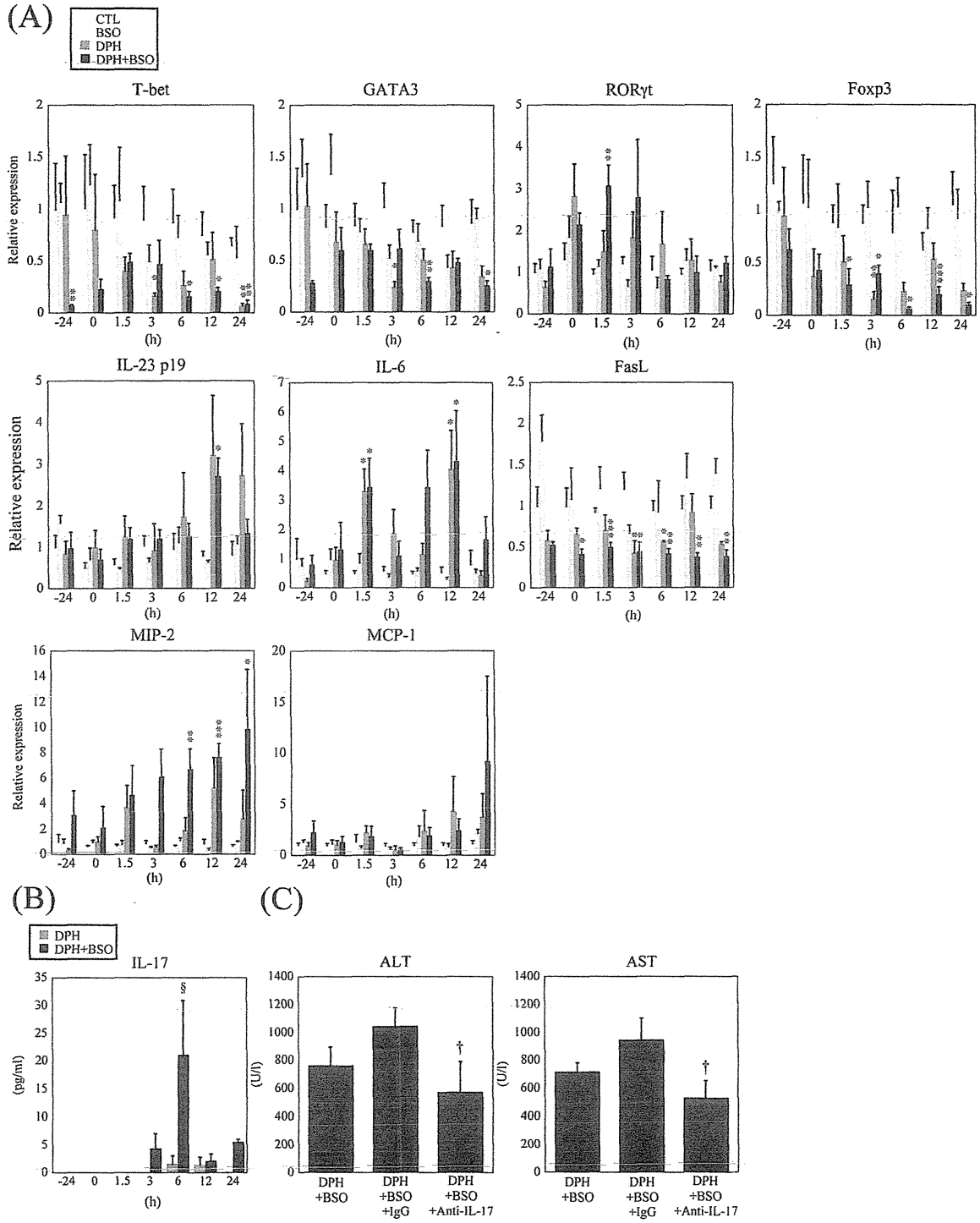

FIG. 6. Time-dependent changes in the hepatic mRNA expression levels and plasma protein levels and a neutralization study of proinflammatory cytokines and chemokines in DPH-induced liver injury. A and B, The experimental conditions for DPH treatments and blood and liver collection were the same as those in Figure 4. C, For the neutralization study, mice were IV injected with an anti-mouse IL-17 antibody (100 μg anti-mouse IL-17 antibody in 0.2 ml of sterile PBS) 3 h after the final DPH treatment. As a control, the IgG isotype was used. At 24 h after the final DPH treatment, plasma was collected to measure its ALT and AST levels. The data are shown as the mean ± SEM. The results of the time-dependent study are taken from 3 to 5 mice, and the results from the neutralization study are taken from 4 to 5 mice. The differences relative to the control mice were considered significant at $*p < .05$, $**p < .01$, and $***p < .001$; –24 h mice were considered significant §$p < .05$ in ELISA; and those compared with isotype IgG-treated mice were considered significant at †$p < .05$ in neutralization study. Abbreviations: ALT, alanine aminotransferase; AST, aspartate aminotransferase; DPH, 5,5-diphenylhydantoin; IL, interleukin; mRNA, messenger RNA.

performed a neutralization study. A monoclonal anti-mouse IL-17 antibody was IV injected 3 h after the final DPH treatment. As a result, the plasma ALT and AST levels were significantly decreased 24 h after the final DPH treatment compared with the levels in mice given an isotype IgG control antibody (Fig. 6C).

The Effect of Prostaglandin E_1 on Liver Injury

PGEs are known to protect against drug-induced and immune-mediated liver injury by downregulating the production of inflammatory cytokines. To investigate the therapeutic effect of PGE_1 on DPH-induced liver injury, PGE_1 conjugated with α-cyclodextrin was IP administered to mice 3 h after the final DPH treatment according to the previously reported method (Higuchi *et al.*, 2012; Kobayashi *et al.*, 2009). The plasma ALT and AST levels were significantly decreased in mice treated with both DPH and BSO compared with the vehicle-treated mice (Fig. 7A). In addition, 24 h after the final DPH treatment (Fig. 7B), PGE_1 treatment significantly decreased the hepatic MIP-2 mRNA levels, whereas the MCP-1 mRNA levels showed a tendency to decrease compared with the vehicle-treated mice. The mRNA expression levels of IL-6 and IL-23 p19 were not significantly changed by PGE_1 (data not shown) because these mRNA expressions were not changed 24 h after the final DPH treatment. In the histopathological evaluation study, PGE_1 treatment significantly decreased the number of MPO-positive cells (Figs. 7C and D). These results suggest that PGE_1 inhibits neutrophil infiltration, likely due to the suppression of Th17 cell function.

DISCUSSION

Development of an understanding of the mechanism of drug-induced liver injury has been hampered by the lack of a suitable animal model. In this study, we first developed a model for DPH-induced liver injury in mice. In particular, we examined different conditions such as the dose of DPH, the number of doses, the dosing method, and the addition of BSO. We succeeded in developing the mouse model for DPH-induced liver injury by administering DPH at 50 mg/kg (IP, approximately one-sixth of the IP LD_{50}) DPH plus BSO for 2 days followed by a dose of 100 mg/kg (p.o., approximately one-seventh of the oral LD_{50}) plus BSO for 3 days. The mice given this treatment showed marked hepatotoxicity (Figs. 1A and D).

DPH is metabolized into an arene oxide and a catechol metabolite in human liver microsomes, suggesting that reactive metabolites are likely implicated in hepatotoxicity (Munns *et al.*, 1997). There are a number of reports showing that BSO, when given together with a drug that causes liver injury in humans, will also cause drug-induced liver injury mouse and rat models (Shimizu et al., 2009, 2011) because GSH is the major antioxidant agent and is protective against toxicity by reactive metabolites or ROS. BSO is a specific inhibitor of γ-glutamylcysteine synthetase, a rate-limiting enzyme involved in GSH synthesis, and it can decrease GSH levels *in vivo* and *in vitro* (Watanabe *et al.*, 2003). In addition, BSO was shown to have no effect on the expression levels of microsomal CYPs and phase II conjugating enzymes such as glutathione-*S*-transferase (GST), sulfotransferase, and uridine diphosphate-glucuronosyltransferase (Drew and Miners, 1984; Griffith and Meister, 1979; Watanabe *et al.*, 2003). Therefore, we adapted a BSO combination method to deplete hepatic GSH. In this study, BSO was administered at a dose of 700 mg/kg 1 h prior to DPH treatment as described in previous studies (Shimizu et al., 2009, 2011). DPH treatment resulted in only a weak hepatotoxicity characterized by the elevation of plasma ALT levels, suggesting that GSH depletion likely exacerbates DPH-induced hepatotoxicity (Fig. 1A). These results indicate that GSH depletion is one of the risk factors for DPH-induced liver injury.

It has been reported that ROS generation is involved in drug-induced hepatotoxicity as reported in nimesulide (Ong *et al.*, 2006). Nimesulide causes mitochondrial impairment, as reflected by the decreasing mitochondrial ATP content and cytochrome C release. Therefore, we think that direct mitochondrial impairment, which is protected against by GSH, is partly involved in DPH-induced liver injury. In the histopathological analysis, apoptotic cells were observed, which might be partly caused by mitochondrial impairment (Fig. 1D).

P450 inhibitors suppressed the covalent binding of a DPH intermediate, and inducers of P450 enhanced the covalent bonding in hepatic microsomes taken from A/J mice (Roy and Snodgrass, 1990). Furthermore, GSH may modulate DPH metabolism either by trapping a DPH-reactive intermediate and decreasing the protein binding or by protecting proteins from attack by electrophilic or free radical intermediates of DPH (Roy and Snodgrass, 1990). Together, these studies and our data indicate that CYP-mediated covalent binding to hepatic proteins may be one of the mechanisms causing DPH-induced liver injury.

Administration of DPH without BSO results in a weak hepatotoxicity compared with a co-treatment with BSO, possibly due to the detoxification of reactive metabolites by GSH under normal conditions (Fig. 1A). Indeed, the administration of DPH caused significant decreases in hepatic GSH levels (Fig. 2A). The decrease in hepatic GSH content was more persistent in the mice treated with DPH plus BSO than in those treated with DPH only, and it could be that sustained reduction in GSH levels is important for toxicity.

The single administration study, even in combination with BSO, resulted in no hepatotoxicity, suggesting that the repeated administration of DPH is necessary for DPH-induced liver injury (Fig. 1B). DPH induces CYP3A4 and CYP2C9 in humans (Chaudhry *et al.*, 2010; Fleishaker *et al.*, 1995) and Cyp3a11 and Cyp2c29 in mice (Hagemeyer *et al.*, 2010), and these CYPs are involved in DPH oxidative metabolism. Therefore, the activation of DPH-inducible Cyps likely precedes

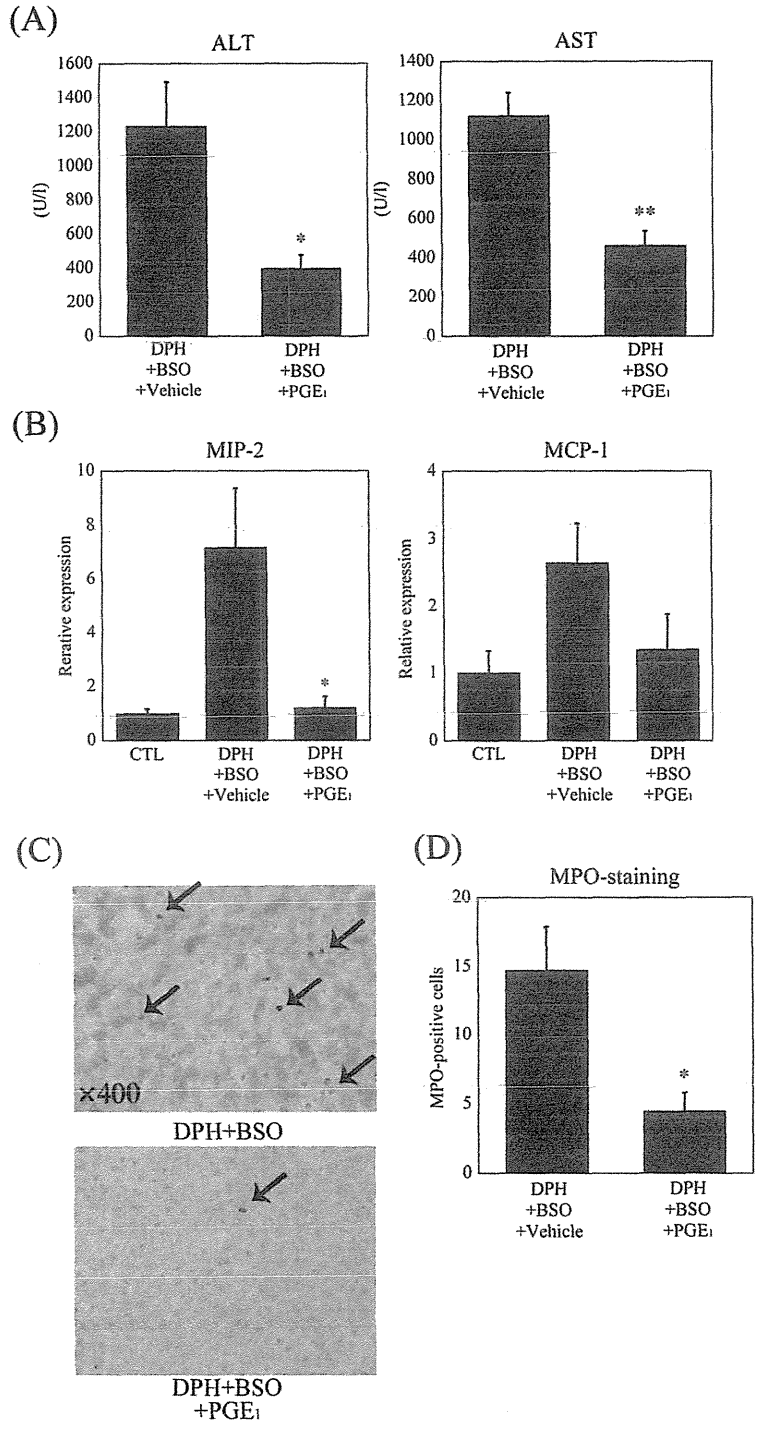

FIG. 7. Effects of PGE_1 on DPH-induced liver injury. The experimental conditions for DPH administration were the same as those in Figure 4. Mice were IP injected with PGE_1 (50 μg/mouse, dissolved in 0.5 ml sterile saline) 3 h after the final DPH treatment. Each vehicle was used as a control. At 24 h after the final DPH treatment, the plasma and liver were collected to measure the ALT and AST levels (A), the hepatic mRNA levels of MIP-2 and MCP-1 (B), and for immunohistochemistry (C and D). The expression level of hepatic mRNA was normalized to that of Gapdh. Mononuclear cell infiltration was assessed by immunostaining for MPO. The number of MPO-positive cells in DPH and BSO-treated or DPH, BSO, and PGE_1-treated mice is shown in (D). The arrows indicate MPO-positive cells. The data are shown as the mean ± SEM of the results from 4 to 5 mice. The differences compared with the DPH-treated, BSO-treated, and vehicle-treated mice were considered significant at $*p < .05$ and $**p < .01$. Abbreviations: ALT, alanine aminotransferase; AST, aspartate aminotransferase; BSO, L-buthionine-S,R-sulfoximine; DPH, 5,5-diphenylhydantoin; MCP-1, monocyte chemoattractant protein-1; MIP-2, macrophage inflammatory protein-2; MPO, myeloperoxidase; mRNA, messenger RNA; PGE_1, Prostaglandin E_1.

the onset of DPH-induced liver injury. During repeated dosing with DPH, even with BSO, no increase in ALT levels was observed on days 1–3 (Fig. 1A). We speculate that the quantity of DPH-inducible Cyps on the fourth day is sufficient to produce the reactive metabolites required for the development of liver injury. Pretreatment with ABT, a nonspecific inhibitor of P450 that can reduce the oxidative metabolism of drugs *in vivo* without any overt toxicity (Shimizu *et al.*, 2009), on the fifth day significantly suppressed the elevation of the ALT levels and the hepatic GSH depletion by DPH plus BSO (Fig. 3A). These data also indicate that P450-mediated metabolism is involved in DPH-induced liver injury.

Previous studies on DPH-induced liver injury in humans show severe hepatocellular injury with a prominent inflammatory response and massive necrosis (Mullick and Ishak, 1980). In this study, hepatic apoptosis, ballooning cells, and neutrophil infiltration were observed in DPH-induced liver injury in mice (Fig. 1D). Necrotic or apoptotic cells trigger a release of cell contents, and as a result, some of the released endogenous compounds are able to activate innate immune cells (Scaffidi *et al.*, 2002). HMGB1 is one of the first DAMPs identified, which is released during endogenous tissue trauma. However, a large number of other molecules, including heat shock proteins, S100A8/9, DNA, RNA, and others, can also function as DAMPs (Bianchi, 2007). The activation of innate immune cells by DAMPs occurs through TLRs, which recognize various molecular patterns including one in HMGB1 (Schwabe *et al.*, 2006).

Mature IL-1β protein is produced by cleavage of precursor IL-1β by caspase-1. The release of active IL-1β engages cells containing IL-1R and promotes inflammatory responses (Bryant and Fitzgerald, 2009; Latz, 2010). Therefore, we thought that IL-1β protein levels do not reflect the mRNA expression levels of IL-1β. Indeed, the mRNA levels of IL-1β were similar between DPH plus BSO-treated and DPH-treated mice, whereas the plasma IL-1β protein levels were significantly increased in DPH plus BSO-treated mice. As reviewed in Latz (2010), Schroder and Tschopp (2010), and Scaffidi *et al.*, 2002), the NALP3 inflammasome is activated by DAMPs that are released from injured cells. The NALP3 inflammasome generates mature IL-1β via proteolytic pathways. Recently, oxidative stress has been shown to play an important role in the activation of the NALP3 inflammasome (Bryant and Fitzgerald, 2009; Martinon *et al.*, 2009; Zhou *et al.*, 2010). In this study, DPH and BSO together significantly increased an oxidative stress marker, the protein carbonyl, suggesting that DPH-generated oxidative stress may be involved in the activation of the NALP3 inflammasome (Fig. 2B).

On the basis of our results, we speculate that the secretion of DAMPs from cells that are injured by reactive metabolites or ROS results in the activation of the NALP3 inflammasome and TLR4 signaling; these processes are factors in the early onset of liver injury because their mRNA levels were increased at relatively early time points. Additionally, we showed that HMGB1 and TLR4 are involved in DPH-induced liver injury (Figs. 4B and C).

Although the mechanism of drug-induced liver injury is still unclear due to the lack of animal models, LPS (lipopolysaccharide)-treated rodent models showed high sensitivity to human hepatotoxic drugs, such as trovafloxacin (Shaw *et al.*, 2009). LPS can activate innate immune responses via TLR4, which might suggest that the susceptibility to innate immune responses is one of the risk factors of DPH-induced liver injury.

In an adaptive immune reaction, Th17 cells may be involved in some types of drug-induced liver injury (Higuchi *et al.*, 2012; Kobayashi *et al.*, 2009). IL-1β and IL-6 or IL-1β together with IL-23 induce Th17 cell differentiation (Acosta-Rodriguez *et al.*, 2007). IL-17, which is produced mainly by a specific subset of Th17 cells, stimulates the production of CXC chemokines such as MIP-2 and plays an important role in neutrophil activity (Langrish *et al.*, 2005; Steinman, 2007). IL-17 is involved in autoimmune responses and some immune-mediated drug-induced liver injuries in mice (Higuchi *et al.*, 2012; Kobayashi *et al.*, 2009). These findings prompted us to investigate the involvement of IL-17 in DPH-induced liver injury. The neutralization of IL-17 significantly inhibited the previously increased plasma ALT and AST levels, suggesting that IL-17 is involved in DPH-induced liver injury (Fig. 6B).

A previous study showed that PGE_1 inhibited neutrophil superoxide production (Talpain *et al.*, 1995) and had a protective effect against drug-induced liver injury in mice. For mice with halothane- and carbamazepine-induced liver injuries, PGE_1 inhibits the increased plasma ALT and IL-17 levels, as well as the expression levels of hepatic MIP-2, IL-6, and IL-23 p19, suggesting that PGE_1 has a protective effect on IL-17-mediated liver injury (Higuchi *et al.*, 2012; Kobayashi *et al.*, 2009). In this study, the elevation of plasma ALT and AST levels, hepatic MIP-2 mRNA expression levels, and the number of hepatic MPO-positive cells were significantly inhibited by PGE_1 (Figs. 7A–C). As a result, we conclude that PGE_1 may be used for pharmacotherapy in DPH-induced liver injury.

In conclusion, in this study, we first established DPH-induced liver injury in mice. We demonstrated that DPH-induced liver injury is related to hepatic GSH levels, oxidative metabolism by Cyps, the innate immune response, and Th17 cell-mediated inflammation. These observations may aid in understanding the risk factors for and the mechanism of the idiosyncratic hepatotoxicity of DPH in humans.

FUNDING

Health and Labor Sciences Research Grants from the Ministry of Health, Labor and Welfare of Japan (H24-BIO-G001).

REFERENCES

Acosta-Rodriguez, E. V., Napolitani, G., Lanzavecchia, A., and Sallusto, F. (2007). Interleukins 1beta and 6 but not transforming growth factor-beta are essential for the differentiation of interleukin 17-producing human T helper cells. *Nat. Immunol.* **8**, 942–949.

Bianchi, M. E. (2007). DAMPs, PAMPs and alarmins: All we need to know about danger. *J. Leukoc. Biol.* **81,** 1–5.

Bryant, C., and Fitzgerald, K. A. (2009). Molecular mechanisms involved in inflammasome activation. *Trends Cell Biol.* **19,** 455–464.

Chaudhry, A. S., Urban, T. J., Lamba, J. K., Birnbaum, A. K., Remmel, R. P., Subramanian, M., Strom, S., You, J. H., Kasperaviciute, D., Catarino, C. B., *et al.* (2010). CYP2C9*1B promoter polymorphisms, in linkage with CYP2C19*2, affect phenytoin autoinduction of clearance and maintenance dose. *J. Pharmacol. Exp. Ther.* **332,** 599–611.

Cuttle, L., Munns, A. J., Hogg, N. A., Scott, J. R., Hooper, W. D., Dickinson, R. G., and Gillam, E. M. (2000). Phenytoin metabolism by human cytochrome P450: involvement of P450 3A and 2C forms in secondary metabolism and drug-protein adduct formation. *Drug Metab. Dispos.* **28,** 945–950.

Dhar, G. J., Pierach, C. A., Ahamed, P. N., and Howard, R. B. (1974). Diphenylhydantoin–induced hepatic necrosis. *Postgrad. Med.* **56,** 128–134.

Drew, R., and Miners, J. O. (1984). The effects of buthionine sulphoximine (BSO) on glutathione depletion and xenobiotic biotransformation. *Biochem. Pharmacol.* **33,** 2989–2994.

Fleishaker, J. C., Pearson, L. K., and Peters, G. R. (1995). Phenytoin causes a rapid increase in 6 beta-hydroxycortisol urinary excretion in humans–A putative measure of CYP3A induction. *J. Pharm. Sci.* **84,** 292–294.

Griffith, O. W., and Meister, A. (1979). Potent and specific inhibition of glutathione synthesis by buthionine sulfoximine (S-n-butyl homocysteine sulfoximine). *J. Biol. Chem.* **254,** 7558–7560.

Hagemeyer, C. E., Bürck, C., Schwab, R., Knoth, R., and Meyer, R. P. (2010). 7-Benzyloxyresorufin-O-dealkylase activity as a marker for measuring cytochrome P450 CYP3A induction in mouse liver. *Anal. Biochem.* **398,** 104–111.

Haruda, F. (1979). Phenytoin hypersensitivity: 38 cases. *Neurology* **29,** 1480–1485.

Higuchi, S., Yano, A., Takai, S., Tsuneyama, K., Fukami, T., Nakajima, M., and Yokoi, T. (2012). Metabolic activation and inflammation reactions involved in carbamazepine-induced liver injury. *Toxicol. Sci.* **130,** 4–16.

Kidd, P. (2003). Th1/Th2 balance: The hypothesis, its limitations, and implications for health and disease. *Altern. Med. Rev.* **8,** 223–246.

Kita, H., Mackay, I. R., Van De Water, J., and Gershwin, M. E. (2001). The lymphoid liver: Considerations on pathways to autoimmune injury. *Gastroenterology* **120,** 1485–1501.

Kobayashi, E., Kobayashi, M., Tsuneyama, K., Fukami, T., Nakajima, M., and Yokoi, T. (2009). Halothane-induced liver injury is mediated by interleukin-17 in mice. *Toxicol. Sci.* **111,** 302–310.

Kobayashi, M., Higuchi, S., Ide, M., Nishikawa, S., Fukami, T., Nakajima, M., and Yokoi, T. (2012). Th2 cytokine-mediated methimazole-induced acute liver injury in mice. *J. Appl. Toxicol.* **32,** 823–833.

Langrish, C. L., Chen, Y., Blumenschein, W. M., Mattson, J., Basham, B., Sedgwick, J. D., McClanahan, T., Kastelein, R. A., and Cua, D. J. (2005). IL-23 drives a pathogenic T cell population that induces autoimmune inflammation. *J. Exp. Med.* **201,** 233–240.

Latz, E. (2010). The inflammasomes: Mechanisms of activation and function. *Curr. Opin. Immunol.* **22,** 28–33.

Martinon, F., Mayor, A., and Tschopp, J. (2009). The inflammasomes: Guardians of the body. *Annu. Rev. Immunol.* **27,** 229–265.

Mullick, F. G., and Ishak, K. G. (1980). Hepatic injury associated with diphenylhydantoin therapy. A clinicopathologic study of 20 cases. *Am. J. Clin. Pathol.* **74,** 442–452.

Munns, A. J., De Voss, J. J., Hooper, W. D., Dickinson, R. G., and Gillam, E. M. (1997). Bioactivation of phenytoin by human cytochrome P450: Characterization of the mechanism and targets of covalent adduct formation. *Chem. Res. Toxicol.* **10,** 1049–1058.

Ong, M. M., Wang, A. S., Leow, K. Y., Khoo, Y. M., and Boelsterli, U. A. (2006). Nimesulide-induced hepatic mitochondrial injury in heterozygous Sod2(+/-) mice. *Free Radic. Biol. Med.* **40,** 420–429.

Oo, Y. H., and Adams, D. H. (2010). The role of chemokines in the recruitment of lymphocytes to the liver. *J. Autoimmun.* **34,** 45–54.

Roy, D., and Snodgrass, W. R. (1990). Covalent binding of phenytoin to protein and modulation of phenytoin metabolism by thiols in A/J mouse liver microsomes. *J. Pharmacol. Exp. Ther.* **252,** 895–900.

Scaffidi, P., Misteli, T., and Bianchi, M. E. (2002). Release of chromatin protein HMGB1 by necrotic cells triggers inflammation. *Nature* **418,** 191–195.

Schroder, K., and Tschopp, J. (2010). The inflammasomes. *Cell* **140,** 821–832.

Schwabe, R. F., Seki, E., and Brenner, D. A. (2006). Toll-like receptor signaling in the liver. *Gastroenterology* **130,** 1886–1900.

Shaw, P. J., Ditewig, A. C., Waring, J. F., Liguori, M. J., Blomme, E. A., Ganey, P. E., and Roth, R. A. (2009). Coexposure of mice to trovafloxacin and lipopolysaccharide, a model of idiosyncratic hepatotoxicity, results in a unique gene expression profile and interferon gamma-dependent liver injury. *Toxicol. Sci.* **107,** 270–280.

Shimizu, S., Atsumi, R., Itokawa, K., Iwasaki, M., Aoki, T., Ono, C., Izumi, T., Sudo, K., and Okazaki, O. (2009). Metabolism-dependent hepatotoxicity of amodiaquine in glutathione-depleted mice. *Arch. Toxicol.* **83,** 701–707.

Shimizu, S., Atsumi, R., Nakazawa, T., Izumi, T., Sudo, K., Okazaki, O., and Saji, H. (2011). Ticlopidine-induced hepatotoxicity in a GSH-depleted rat model. *Arch. Toxicol.* **85,** 347–353.

Spielberg, S. P., Gordon, G. B., Blake, D. A., Goldstein, D. A., and Herlong, H. F. (1981). Predisposition to phenytoin hepatotoxicity assessed in vitro. *N. Engl. J. Med.* **305,** 722–727.

Steinman, L. (2007). A brief history of T(H)17, the first major revision in the T(H)1/T(H)2 hypothesis of T cell-mediated tissue damage. *Nat. Med.* **13,** 139–145.

Talpain, E., Armstrong, R. A., Coleman, R. A., and Vardey, C. J. (1995). Characterization of the PGE receptor subtype mediating inhibition of superoxide production in human neutrophils. *Br. J. Pharmacol.* **114,** 1459–1465.

Taylor, J. W., Stein, M. N., Murphy, M. J., and Mitros, F. A. (1984). Cholestatic liver dysfunction after long-term phenytoin therapy. *Arch. Neurol.* **41,** 500–501.

Tietze, F. (1969). Enzymic method for quantitative determination of nanogram amounts of total and oxidized glutathione: Applications to mammalian blood and other tissues. *Anal. Biochem.* **27,** 502–522.

Watanabe, T., Sagisaka, H., Arakawa, S., Shibaya, Y., Watanabe, M., Igarashi, I., Tanaka, K., Totsuka, S., Takasaki, W., and Manabe, S. (2003). A novel model of continuous depletion of glutathione in mice treated with L-buthionine (S,R)-sulfoximine. *J. Toxicol. Sci.* **28,** 455–469.

Winn, L. M., and Wells, P. G. (1995). Phenytoin-initiated DNA oxidation in murine embryo culture, and embryo protection by the antioxidative enzymes superoxide dismutase and catalase: Evidence for reactive oxygen species-mediated DNA oxidation in the molecular mechanism of phenytoin teratogenicity. *Mol. Pharmacol.* **48,** 112–120.

Winn, L. M., and Wells, P. G. (1999). Maternal administration of superoxide dismutase and catalase in phenytoin teratogenicity. *Free Radic. Biol. Med.* **26,** 266–274.

Yamazaki, H., Komatsu, T., Takemoto, K., Saeki, M., Minami, Y., Kawaguchi, Y., Shimada, N., Nakajima, M., and Yokoi, T. (2001). Decreases in phenytoin hydroxylation activities catalyzed by liver microsomal cytochrome P450 enzymes in phenytoin-treated rats. *Drug Metab. Dispos.* **29,** 427–434.

Zhou, R., Tardivel, A., Thorens, B., Choi, I., and Tschopp, J. (2010). Thioredoxin-interacting protein links oxidative stress to inflammasome activation. *Nat. Immunol.* **11,** 136–140.

Zimmerman, H. J. (1999). *Hepatotoxicity: The Adverse Effects of Drugs and Other Chemicals on the Liver.* Lippncott Williams & Wilkins, Philadelphia, PA.

Toxicology and Applied Pharmacology 272 (2013) 154–160

Contents lists available at ScienceDirect

Toxicology and Applied Pharmacology

journal homepage: www.elsevier.com/locate/ytaap

Cigarette smoking substantially alters plasma microRNA profiles in healthy subjects

Kei Takahashi [1], Shin-ichi Yokota [1], Naoyuki Tatsumi, Tatsuki Fukami, Tsuyoshi Yokoi, Miki Nakajima *

Drug Metabolism and Toxicology, Faculty of Pharmaceutical Sciences, Kanazawa University, Kakuma-machi, Kanazawa 920-1192, Japan

ARTICLE INFO

Article history:
Received 16 March 2013
Revised 16 May 2013
Accepted 18 May 2013
Available online 29 May 2013

Keywords:
MicroRNA
Smoking
Biomarker

ABSTRACT

Circulating microRNAs (miRNAs) are receiving attention as potential biomarkers of various diseases, including cancers, chronic obstructive pulmonary disease, and cardiovascular disease. However, it is unknown whether the levels of circulating miRNAs in a healthy subject might vary with external factors in daily life. In this study, we investigated whether cigarette smoking, a habit that has spread throughout the world and is a risk factor for various diseases, affects plasma miRNA profiles. We determined the profiles of 11 smokers and 7 non-smokers by TaqMan MicroRNA array analysis. A larger number of miRNAs were detected in smokers than in non-smokers, and the plasma levels of two-thirds of the detected miRNAs (43 miRNAs) were significantly higher in smokers than in non-smokers. A principal component analysis of the plasma miRNA profiles clearly separated smokers and non-smokers. Twenty-four of the miRNAs were previously reported to be potential biomarkers of disease, suggesting the possibility that smoking status might interfere with the diagnosis of disease. Interestingly, we found that quitting smoking altered the plasma miRNA profiles to resemble those of non-smokers. These results suggested that the differences in the plasma miRNA profiles between smokers and non-smokers could be attributed to cigarette smoking. In addition, we found that an acute exposure of ex-smokers to cigarette smoke (smoking one cigarette) did not cause a dramatic change in the plasma miRNA profile. In conclusion, we found that repeated cigarette smoking substantially alters the plasma miRNA profile, interfering with the diagnosis of disease or signaling potential smoking-related diseases.

Introduction

MicroRNAs (miRNAs) are a class of endogenous, short non-coding RNAs 19–25 nucleotides in length that negatively regulate gene expression via translational repression or mRNA degradation, primarily by pairing with the 3′-untranslated regions of the target mRNAs (Ambros, 2001). More than 2,000 human miRNAs have been identified (miRBase ver. 19). It is now clear that miRNAs are involved in various important biological processes, including cell differentiation, proliferation, apoptosis, and development (He and Hannon, 2004; Meltzer, 2005). Some miRNAs are expressed in a tissue-specific manner, and others are ubiquitously expressed (Liang et al., 2007). It is also known that miRNA expression is significantly altered in several diseases (http://www.miR2disease.org/), and the dysregulation of miRNAs is closely linked with the incidence or progress of these diseases.

It was reported in 2008 that miRNAs exist in plasma or serum (Mitchell et al., 2008). Subsequent reports have revealed the presence of miRNAs in saliva (Michael et al., 2010; Park et al., 2009) and urine (Hanke et al., 2010). These extracellular miRNAs are stable in the RNase-rich environment because they are enclosed in vesicles, including exosomes, microvesicles, apoptotic bodies, and ectosomes (Lee et al., 2012), or are associated with RNA-binding proteins, including nucleophosmin 1 (Wang et al., 2010b) or high-density lipoprotein (Vickers et al., 2011). Following the discovery of extracellular miRNA in body fluids, a significant number of papers reported that the levels of some extracellular miRNAs are linked to different pathophysiological conditions. Examples of this include the associations of miR-141 and miR-375 with prostate cancer (Bryant et al., 2012), miR-29a and miR-92a with colorectal cancer (Huang et al., 2010), miR-499 with myocardial infarction (Olivieri et al., in press), and miR-122 with liver injury (Wang et al., 2009). These findings introduce the possibility of using the levels of specific miRNAs in body fluids as biomarkers for different pathological conditions (Duttagupta et al., 2011; Wang et al., 2012b). However, it is unknown whether the levels of extracellular miRNAs in a healthy subject might vary with external factors in daily life.

Cigarette smoking is a habit that has spread all over the world and is a significant risk factor for many diseases, including lung cancer (Shields, 1999), chronic obstructive pulmonary disease (Higgins et al., 1984), asthma (Ulrik and Lange, 2001) and cardiovascular disease (Holbrook et al., 1984). Cigarette smoke contains over 4800 chemicals, including 69 carcinogens (Hoffmann et al., 2001), which appear to be of crucial importance in causing disease. We questioned whether cigarette smoking alters plasma miRNA

* Corresponding author. Fax: +81 76 234 4407.
E-mail address: nmiki@p.kanazawa-u.ac.jp (M. Nakajima).
[1] K.T. and S.Y. contributed equally to this work.

0041-008X/$ – see front matter © 2013 Elsevier Inc. All rights reserved.
http://dx.doi.org/10.1016/j.taap.2013.05.018

profiles in humans, and, if it does, whether the changes may be associated with the pathogenesis of various diseases. In this study, we compared the plasma miRNA profiles of smokers and non-smokers and discussed the biological significance of the different profiles by the smoking status.

Materials and methods

Chemicals and reagents. The *mir*Vana PARIS Kit, Megaplex pools, TaqMan microRNA Reverse Transcription Kit, TaqMan Universal PCR Master Mix (No AmpErase UNG) and TaqMan Human MicroRNA Array A and B Card v2.0 were from Life Technologies (Carlsbad, CA). Nicotine and cotinine were purchased from Sigma (St. Louis, MO). Acetanilide was purchased from Wako (Osaka, Japan). All other chemicals and solvents were of the highest grade commercially available.

Study design. This study was approved by the Ethics Committee of Kanazawa University (Kanazawa, Japan). Written, informed consent was obtained from all the subjects. Eleven smokers (S1–S11) and seven non-smokers (NS1–NS7) who were healthy male Japanese taking no medicines or supplements were recruited (Table 1). The smokers smoked their favorite brands of cigarettes as shown in Table 1. The pack year (number of cigarettes per day × number of years smoked/20 cigarettes in one pack) ranged from 4 to 35 (18 ± 9). There were no significant differences in the age and body weight of the smokers and non-smokers.

This study consists of three experiments. For the blood collection (5 ml), subjects came at 10 AM without having had breakfast. In experiment I, blood was collected from all subjects to compare the plasma miRNA profiles in smokers and non-smokers. Smoking occurred in the morning or not, according to each smoker's habit. After experiment I, we noticed that four smokers (S1, S2, S4, and S8) had voluntarily quit smoking. Among them, subject S8 had used nicotine patches after experiment I. In experiment II, blood was collected from the four subjects to determine their plasma miRNA profiles after they quit smoking (S1, S2, and S4 were tested one month after quitting; S8 was tested three months after quitting but was using nicotine patches). After that, two subjects, S1 and S4, returned to smoking. We had asked them to contact us when they began smoking again. In experiment III, blood was collected from the two subjects (S1 and S4) 20 min after they smoked the first cigarette (Mild Seven, Japan Tobacco, Tokyo, Japan) to determine the plasma miRNA profiles immediately after exposure to cigarette smoke.

RNA isolation from plasma. Ethylenediamine-*N,N,N′,N′*-tetraacetic acid disodium salt was added as an anticoagulant to the blood, which was then kept at room temperature for 30 min. After centrifugation at 3000 *g* for 10 min at 4 °C, the plasma was collected. Immediately, total RNA was isolated from 600 μl of plasma using the *mir*Vana PARIS kit as described previously (Yamaura et al., 2012).

Taqman microRNA array analysis. The expression profiles of miRNAs were assessed using TaqMan Human MicroRNA Array A + B Cards Sets v2.0 containing 377 (A array) or 287 (B array) primer-probe sets for individual miRNAs (total 664 miRNAs). All procedures were performed following the manufacturer's instructions. Briefly, 3 μl of total RNA was reverse transcribed using Megaplex RT Primer Pool A or B and TaqMan MicroRNA Reverse Transcription Kits. Pre-amplification was carried out using Megaplex PreAmp primers and the TaqMan PreAmp Master Mix. The expression of miRNAs was determined by quantitative real-time PCR using the TaqMan Human MicroRNA Array with the 7900HT Fast Real-Time PCR System (Life Technologies) and the manufacturer's recommended cycling conditions. Cycle threshold (Ct) values were calculated using the SDS software v.2.3 with a baseline of 3–15 and an assigned minimum threshold of 0.2. Expression of miRNAs was normalized by global normalization, which implicitly assumes that the mean expression level of all monitored miRNAs is constant. Any miRNA giving 40-Ct < 8, a cutoff value recommended by the manufacturer, in at least one sample was omitted from the data analysis.

Principal component analysis. The plasma miRNA expression data were analyzed using the Partek Genomics Suite version 6.12 (Partek, St. Louis, MO). Principal component analysis (PCA) was performed to visualize the difference between groups of the expression profiles of miRNAs that exceeded the cutoff value.

Measurement of plasma concentrations of nicotine and cotinine. Plasma concentrations of nicotine and cotinine were measured as described previously (Nakajima et al., 2000) with slight modifications. The plasma sample (0.5 ml) was alkalinized with 25 μl of 10 M NaOH. After the addition of 10 μl of 7 μM acetanilide as an internal standard, the mixture was extracted with 4 ml dichloromethane by shaking for 10 min.

Table 1
Characteristics of subjects.

Subject	Age (years)	Height (cm)	Body weight (kg)	Brand of cigarette	Nicotine (mg)	Tar (mg)	Age at starting smoking (years)	Number of cigarettes per day	Number of years smoked (years)	Pack-year
S1	36	168	50	Mild Seven	0.7	8	20	15	16	12
S2	41	170	64	Mild Seven Lights	0.7	8	20	20	21	21
S3	35	169	65	Mild Seven	0.8	10	20	30	15	23
S4	55	177	68	Marlboro	1.0	12	20	20	35	35
S5	21	172	80	Hi-Lite Menthol	0.7	10	16	15	5	4
S6	46	165	53	Hi-Lite	1.4	17	20	20	26	26
S7	38	167	57	Mild Seven Aqua Menthol	0.1	1	20	10	18	9
S8	37	165	58	Lark Menthol	0.1	1	20	20	17	17
S9	40	156	53	Cabin	0.4	5	18	20	22	22
S10	36	172	55	Mild Seven Super Lights	0.5	6	20	20	16	16
S11	39	168	65	Kool Mild	0.7	8	16	10	23	12
Mean ± SD	38.5 ± 8.2	168 ± 5.0	61.7 ± 8.7		0.6 ± 0.4	8 ± 5		18 ± 6	19 ± 8	18 ± 9
NS1	26	163	65							
NS2	39	177	84							
NS3	50	164	63							
NS4	29	169	62							
NS5	41	173	80							
NS6	43	161	57							
NS7	28	170	67							
Mean ± SD	36.6 ± 9.0	168.1 ± 5.8	68.3 ± 9.9							

After centrifugation at 1000 g for 10 min, 12 μl of 12 M HCl was added to the organic fraction. The organic fraction was evaporated with a vacuum evaporator at 40 °C. The residue was redissolved in 50 μl of the mobile phase, and then a 20 μl portion of the sample was subjected to liquid chromatography/tandem mass spectrometry (LC-MS/MS). The LC-MS/MS condition was described in our previous report (Yamanaka et al., 2004).

Statistical analysis. Data are presented as the mean ± standard deviation. Statistical analyses of the differences between two groups were performed by an unpaired two-tailed Student's *t*-test. A value of *P* less than 0.05 was considered statistically significant.

Results

Plasma miRNA profiles of non-smokers and smokers

We determined plasma miRNA expression in 11 smokers and 7 non-smokers by quantitative real-time PCR using the TaqMan MicroRNA Array. The numbers of miRNAs with 40-Ct > 8 in each individual are shown in Table 2. The numbers in smokers (196 ± 18) were significantly ($P < 0.001$) larger than those in non-smokers (143 ± 29). The number of miRNAs that exceeded the cutoff value in all subjects (n = 18) was 66. We compared the levels of 66 miRNAs in smokers and non-smokers. Among them, 44 miRNAs showed a significant difference between the groups (Table 3). Forty-three miRNAs were higher in smokers than in non-smokers, whereas 1 miRNA was lower in smokers than in non-smokers. To visualize the difference in the expression profiles of miRNAs between smokers and non-smokers, PCA was performed using the expression data for the 66 miRNAs. PC1 encompassed a significantly large proportion (63%) of the total variance for each subject, followed by PC2 (10%) and PC3 (6%). As shown in Fig. 1, the profiles of plasma miRNA expression of the smokers were different from those of the non-smokers.

Quitting smoking altered the plasma miRNA profile

To investigate whether the difference in the plasma miRNA profiles between smokers and non-smokers was due to cigarette smoking, we examined miRNA expression in the plasma of 4 smokers who had stopped smoking (S1, S2, S4, and S8). To confirm their non-smoking status, we measured their plasma concentrations of nicotine and cotinine. For comparison, nicotine and cotinine concentrations were also measured when they were still smoking (experiment I); these concentrations were 3.6–26.0 ng/ml and 23.4–413.0 ng/ml, respectively (Table 4). One month after they stopped smoking, the levels in S1 and S2 had dramatically decreased to values close to the detection limit. In the plasma from S4, low levels of nicotine and cotinine were detected; therefore, he might have been smoking in secret or been exposed to

Table 3
Forty-four plasma miRNAs are differently ($P < 0.05$) expressed in 7 non-smokers (NS) compared to 11 smokers (S).

microRNA	40 - Ct value (Mean ± SD)		Fold (S/NS)	*P*-value
	NS	S		
miR-374b	12.75 ± 2.89	15.76 ± 1.03	8.11	0.006
miR-331-3p	11.72 ± 2.85	14.61 ± 1.26	7.39	0.009
miR-221	12.84 ± 2.46	15.61 ± 1.57	6.83	0.010
let-7g	12.85 ± 1.78	15.40 ± 0.89	5.89	0.001
miR-301a	10.66 ± 1.79	13.09 ± 0.78	5.39	0.001
let-7e	15.47 ± 1.07	17.74 ± 1.13	4.83	0.001
miR-335	11.21 ± 1.94	13.48 ± 0.80	4.83	0.003
miR-26a	14.91 ± 1.45	17.09 ± 0.91	4.51	0.001
miR-30c	15.21 ± 1.13	17.35 ± 0.82	4.40	0.000
miR-185	10.65 ± 2.06	12.77 ± 0.67	4.36	0.005
miR-374a	13.71 ± 1.50	15.83 ± 0.96	4.36	0.002
miR-30b	15.24 ± 1.20	17.36 ± 0.76	4.33	0.000
let-7b	14.33 ± 1.06	16.43 ± 0.94	4.30	0.000
miR-451	15.62 ± 1.75	17.70 ± 1.61	4.22	0.020
miR-27a	12.36 ± 2.02	14.26 ± 0.48	3.74	0.008
miR-29a	12.78 ± 1.32	14.64 ± 0.43	3.63	0.000
miR-191	18.18 ± 1.79	20.04 ± 0.87	3.63	0.009
miR-26b	14.15 ± 1.33	15.99 ± 0.75	3.59	0.002
miR-199a-3p	14.49 ± 1.54	16.30 ± 0.82	3.52	0.005
miR-425	12.11 ± 1.50	13.92 ± 0.78	3.51	0.004
miR-223	21.95 ± 1.59	23.70 ± 0.45	3.36	0.003
miR-328	13.18 ± 1.91	14.87 ± 0.94	3.23	0.023
miR-21	14.41 ± 1.42	16.06 ± 0.38	3.14	0.002
let-7d	13.32 ± 0.94	14.97 ± 0.91	3.12	0.002
miR-19b	18.36 ± 1.39	20.00 ± 0.56	3.12	0.003
miR-106b	13.34 ± 1.71	14.92 ± 0.82	2.99	0.017
miR-19a	14.53 ± 1.29	16.10 ± 0.53	2.96	0.002
miR-186	15.79 ± 1.55	17.33 ± 0.60	2.92	0.008
miR-93	14.99 ± 1.67	16.44 ± 0.73	2.72	0.021
miR-454	14.12 ± 1.00	15.52 ± 0.88	2.64	0.007
miR-345	11.46 ± 1.29	12.86 ± 0.71	2.63	0.009
miR-20b	15.24 ± 1.44	16.60 ± 0.36	2.57	0.008
miR-17	18.67 ± 1.31	19.89 ± 0.50	2.33	0.013
miR-20a	18.08 ± 1.31	19.29 ± 0.58	2.32	0.015
miR-24	18.26 ± 1.58	19.43 ± 0.74	2.25	0.048
miR-106a	18.58 ± 1.43	19.75 ± 0.56	2.25	0.026
miR-126	19.24 ± 1.06	20.41 ± 0.75	2.24	0.015
miR-16	20.12 ± 1.09	21.26 ± 0.78	2.19	0.020
miR-25	13.92 ± 1.18	15.04 ± 0.68	2.18	0.020
miR-923	13.19 ± 1.59	14.31 ± 0.58	2.16	0.016
miR-195	14.69 ± 1.10	15.79 ± 0.91	2.14	0.035
miR-126*	16.28 ± 1.02	17.33 ± 0.58	2.07	0.013
miR-92a	17.36 ± 0.81	18.12 ± 0.64	1.70	0.039
miR-188-5p	12.90 ± 0.95	12.05 ± 0.74	0.55	0.047

Plasma miRNAs shaded with gray have been reported to be candidate biomarkers of diseases (Table 6).

Table 2
The numbers of plasma miRNAs with 40-Ct > 8 in non-smokers (NS) and smokers (S).

Non-smokers		Smokers		Status		
				Smoking	Quit	Acute exposure
NS1	174	S1	198	198	160	177
NS2	191	S2	216	216	138	
NS3	138	S3	208			
NS4	138	S4	234	234	129	131
NS5	110	S5	189			
NS6	121	S6	189			
NS7	129	S7	185			
		S8	187	187	137	
		S9	177			
		S10	170			
		S11	200			
Mean ± SD	143 ± 29	Mean ± SD	196 ± 18***	209 ± 21	141 ± 13##	

*** $P < 0.001$, compared with non-smokers.
$P < 0.01$, compared with smoking status in 4 smokers (S1, S2, S4, and S8).

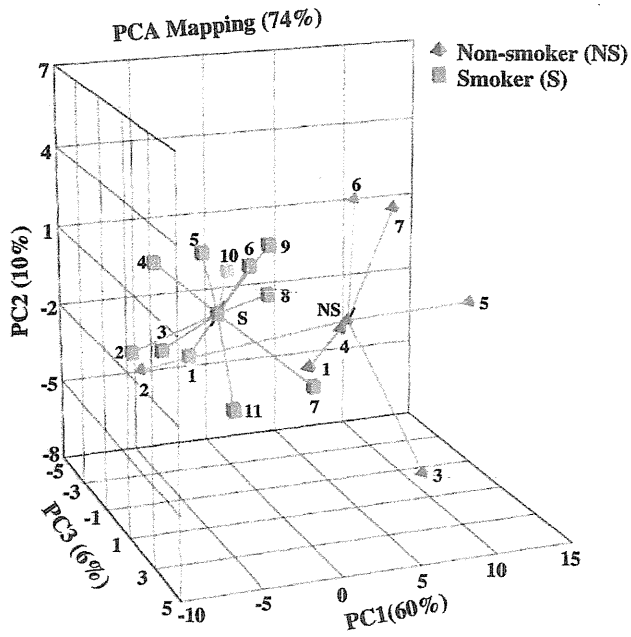

Fig. 1. PCA of plasma miRNA expression in 7 non-smokers (NS) and 11 smokers (S). PCA was performed using 66 miRNAs that exceeded the cutoff value in all subjects (n = 18). A three-component model was developed that explained a total of 79% (PC1, 63%; PC2, 10%; PC3, 6%) of the variability of the data. Each ball representing an individual is connected to the centroid (marked as NS or S) of each group. The numbers near the balls represent the subject number. This plot illustrates the level of spread between individuals and groups using three principal components.

passive smoking. S8 showed substantial nicotine and cotinine levels comparable to those of active smokers. These levels were not surprising because this subject used nicotine patches.

The numbers of miRNAs with 40-Ct > 8 in the 4 subjects who had stopped smoking were 141 ± 13 (129–160). Interestingly, the number was very close to that in non-smokers (143 ± 29) and was significantly ($P < 0.01$) lower than that when they were still smoking (209 ± 21) (Table 2). We compared the plasma miRNA expression in the four subjects before and after they stopped smoking. The numbers of miRNAs that exceeded the cutoff value in the four subjects was 93. Among them, 63 miRNAs showed a significant difference between the groups (Table 5). Sixty miRNAs were significantly lower after the subjects had stopped smoking than before they stopped, whereas 3 miRNAs were significantly higher after they stopped than before they stopped. Interestingly, among the 60 miRNAs that were lower after the subjects had stopped smoking, 38 miRNAs (shaded in Table 5) were the ones more highly expressed in smokers than in non-smokers (Table 2). These results suggested that the plasma miRNA expression is unambiguously affected by smoking.

We considered the possibility that quitting smoking might alter the plasma miRNA profiles to resemble the profiles of non-smokers. To test this possibility, we compared the plasma miRNA profiles of the 4 subjects before and after they stopped smoking, as well as the profiles of the 7 non-smokers. The number of miRNAs exceeding the cutoff value among the three groups was 66. PCA was performed using the expression data of the 66 miRNAs (Fig. 2A). PC1 encompassed the largest

Table 4
Plasma concentrations of nicotine and cotinine in 4 smokers who quit smoking for at least one month and then smoked again.

Smoker	Nicotine (ng/ml)			Cotinine (ng/ml)		
	Status			Status		
	Smoking	Quit	Acute exposure	Smoking	Quit	Acute exposure
S1	3.6	0.1	13.7	282.1	1.1	5.1
S2	16.3	1.0		23.4	0.6	
S4	16.7	3.3	15.7	413.0	9.5	17.9
S8	26.0	25.9		243.5	364.3	

Table 5
Sixty-three plasma miRNAs differently ($P < 0.05$) expressed in 4 subjects (S1, S2, S4, and S8) who smoked (S) and then quit smoking (Q).

microRNA	40-Ct values (Mean ± SD)		Fold (Q/S)	*P*-value
	S	Q		
hsa-miR-766	15.07 ± 1.48	10.44 ± 0.92	0.04	0.002
hsa-miR-374b	16.30 ± 0.47	11.73 ± 0.87	0.04	0.000
hsa-miR-340	13.41 ± 0.32	9.64 ± 1.05	0.07	0.000
hsa-let-7e	18.30 ± 1.06	14.57 ± 0.50	0.08	0.001
hsa-miR-191	20.53 ± 0.80	16.85 ± 0.65	0.08	0.000
hsa-miR-103	13.99 ± 1.22	10.34 ± 1.98	0.08	0.020
hsa-miR-199a-3p	16.67 ± 0.91	13.13 ± 0.46	0.09	0.000
hsa-miR-625*	14.33 ± 1.50	10.83 ± 0.53	0.09	0.005
hsa-miR-186	17.45 ± 0.47	14.01 ± 0.96	0.09	0.001
hsa-let-7g	15.68 ± 0.86	12.25 ± 1.41	0.09	0.006
hsa-miR-185	12.85 ± 0.54	9.43 ± 0.84	0.09	0.000
hsa-miR-197	15.88 ± 0.97	12.52 ± 1.36	0.10	0.007
hsa-miR-331-3p	15.43 ± 0.91	12.19 ± 0.76	0.11	0.002
hsa-miR-454	15.71 ± 0.91	12.50 ± 0.33	0.11	0.001
hsa-miR-374a	16.15 ± 0.49	12.95 ± 0.84	0.11	0.001
hsa-let-7b	16.62 ± 1.04	13.52 ± 0.70	0.12	0.003
hsa-miR-495	12.63 ± 0.42	9.54 ± 0.76	0.12	0.000
hsa-let-7d	15.36 ± 0.78	12.44 ± 0.70	0.13	0.001
hsa-miR-484	19.64 ± 0.80	16.77 ± 0.94	0.14	0.004
hsa-miR-19a	16.28 ± 0.18	13.51 ± 0.99	0.15	0.001
hsa-miR-301a	13.38 ± 0.62	10.65 ± 0.76	0.15	0.001
hsa-miR-26a	17.63 ± 0.70	14.93 ± 0.95	0.15	0.004
hsa-miR-151-3p	15.05 ± 1.23	12.35 ± 0.30	0.15	0.005
hsa-miR-335	13.88 ± 0.77	11.21 ± 0.54	0.16	0.001
hsa-miR-181a	17.87 ± 1.20	9.21 ± 0.84	0.16	0.011
hsa-miR-222	19.08 ± 0.74	16.44 ± 1.15	0.16	0.008
hsa-miR-28-3p	14.60 ± 0.79	11.98 ± 1.10	0.16	0.008
hsa-miR-590-5p	14.43 ± 0.24	11.82 ± 0.26	0.16	0.000
hsa-miR-140-5p	15.85 ± 0.76	13.28 ± 0.67	0.17	0.002
hsa-miR-30b	17.77 ± 0.51	15.20 ± 0.83	0.17	0.002
hsa-miR-30d	12.03 ± 1.26	9.47 ± 0.98	0.17	0.018
hsa-miR-15b	15.56 ± 0.58	13.03 ± 0.78	0.17	0.002
hsa-miR-20b	16.63 ± 0.30	14.14 ± 0.82	0.18	0.001
hsa-miR-93	16.81 ± 0.69	14.38 ± 0.92	0.19	0.006
hsa-miR-223	23.87 ± 0.27	21.45 ± 0.45	0.19	0.000
hsa-miR-342-3p	17.36 ± 0.42	15.00 ± 0.10	0.19	0.007
hsa-miR-320	18.79 ± 0.88	16.45 ± 0.71	0.20	0.006
hsa-miR-28-5p	12.55 ± 0.73	10.23 ± 1.06	0.20	0.011
hsa-miR-328	15.56 ± 0.91	13.25 ± 0.08	0.20	0.002
hsa-miR-24	19.90 ± 0.65	17.63 ± 0.52	0.21	0.002
hsa-miR-126	20.70 ± 0.57	18.57 ± 0.49	0.23	0.001
hsa-miR-26b	16.19 ± 0.33	14.07 ± 0.80	0.23	0.003
hsa-miR-152	12.97 ± 0.65	10.89 ± 0.19	0.24	0.022
hsa-miR-27a	14.50 ± 0.37	12.51 ± 0.29	0.25	0.000
hsa-miR-17	20.04 ± 0.45	18.05 ± 0.65	0.25	0.002
hsa-miR-30c	17.78 ± 0.66	15.82 ± 0.90	0.26	0.013
hsa-miR-19b	20.02 ± 0.28	18.21 ± 0.72	0.28	0.003
hsa-miR-106a	19.90 ± 0.63	18.09 ± 0.39	0.29	0.003
hsa-miR-20a	19.41 ± 0.36	17.61 ± 0.48	0.29	0.001
hsa-miR-923	14.40 ± 0.85	12.66 ± 0.88	0.30	0.030
hsa-miR-29a	14.62 ± 0.48	12.93 ± 0.33	0.31	0.001
hsa-miR-345	13.14 ± 0.88	11.46 ± 0.61	0.31	0.020
hsa-miR-18a	13.32 ± 0.53	11.64 ± 0.23	0.31	0.001
hsa-miR-106b	14.88 ± 0.22	16.42 ± 0.43	0.36	0.001
hsa-miR-16	21.06 ± 0.45	19.60 ± 0.65	0.36	0.010
hsa-miR-126*	17.04 ± 0.35	15.60 ± 0.95	0.37	0.029
hsa-miR-532-5p	12.25 ± 0.76	10.83 ± 0.53	0.37	0.022
hsa-miR-148a	12.15 ± 0.66	10.90 ± 0.78	0.42	0.050
hsa-miR-92a	18.31 ± 0.42	17.07 ± 0.65	0.42	0.019
hsa-miR-21	15.98 ± 0.36	14.81 ± 0.65	0.45	0.020
hsa-miR-135a*	15.80 ± 0.88	17.06 ± 0.39	2.39	0.039
hsa-miR-188-5p	11.68 ± 0.45	13.20 ± 0.12	2.86	0.001
hsa-miR-138-1*	11.61 ± 1.31	14.36 ± 0.21	6.73	0.006

Plasma miRNAs shaded with gray were more highly expressed in smokers than in non-smokers (Table 3).

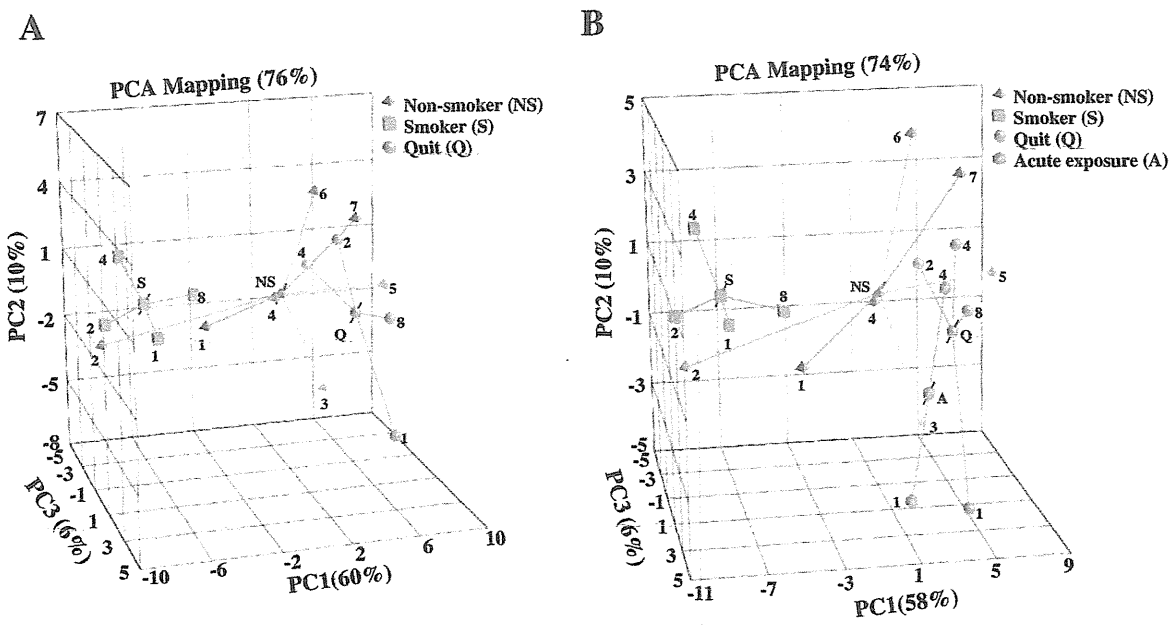

Fig. 2. The effects of quitting smoking and of subsequently smoking one cigarette on plasma miRNA profiles. (A) PCA was performed using 66 miRNAs that exceeded the cutoff value in 4 subjects who smoked and who quit smoking, as well as in 7 non-smokers. A three-component model was developed explaining a total of 76% (PC1, 60%; PC2, 10%; PC3, 6%) of the variability of the data. Each ball representing an individual is connected to the centroid (marked as NS, S, or Q) of each group. The numbers near the balls represent the subject number. (B) PCA for the expression of 66 miRNAs in 4 groups: 4 subjects who smoked and who quit smoking, 7 non-smokers and 2 subjects who quit smoking but then smoked one cigarette. A three-component model was developed explaining a total of 74% (PC1, 58%; PC2, 10%; PC3, 6%) of the variability of the data. Each ball representing an individual is connected to the centroid (marked as NS, S, Q, or A) of each group.

proportion (60%) of the total variance for each subject, followed by PC2 (10%) and PC3 (6%). These results clearly demonstrated that the plasma miRNA profiles of smokers were altered after they stopped smoking, and the profiles then resembled those of non-smokers.

Smoking one cigarette does not cause a dramatic change in the expression of plasma miRNAs

To ascertain how quickly the plasma miRNA profile was changed by smoking, we examined plasma miRNA profiles 20 min after 2 ex-smokers (S1 and S4) had each smoked one cigarette. We chose this time because it is near the Cmax values of nicotine and cotinine after smoking (Yamanaka et al., 2004). The plasma concentrations of nicotine after one cigarette were 13.7 ng/ml and 15.7 ng/ml, and those of cotinine were 5.1 ng/ml and 17.9 ng/ml (Table 4), suggesting that the subjects had inhaled the cigarette smoke. The numbers of miRNAs with 40-Ct > 8 were 177 and 131, slightly larger than the numbers of miRNAs prior to smoking the cigarettes (Table 2). The miRNA expression data were included in the PCA for the 66 miRNAs described above. As shown in Fig. 2B, the miRNA profiles after smoking one cigarette were similar to those of the smokers who had stopped smoking and the non-smokers. These results suggest that changes in the plasma miRNA profiles in smokers might be due to repeated smoking.

Discussion

Circulating miRNAs have received considerable attention as potential biomarkers of various diseases (Reid et al., 2011) based on many studies reporting differences in plasma or serum miRNA levels between healthy subjects and patients. However, it remains unclear to what extent the circulating miRNA profiles in healthy subjects vary in daily life due to changes in diet, supplements, alcohol intake, cigarette smoking, exposure to environmental chemicals, sleeping or circadian rhythm, stress, and exercise or other factors. In the present study, we focused on cigarette smoking because it is a habit spread all over the world and is a significant risk factor for various diseases including cancer. In the present investigation of the plasma miRNA profiles of smokers and non-smokers, the subjects were limited to men because a study had reported subtle sex differences (Ji et al., 2009), although another study reported no large sex differences in plasma miRNA expression (Chen et al., 2008), and because smoking is more prevalent in men than in women in Japan. In addition, considering the potential effects of circadian rhythm (Shende et al., 2011), we standardized the time of blood collection.

We found that a larger number of miRNAs were detected in smokers than in non-smokers, and the plasma levels of two-thirds of the detected miRNAs (43 miRNAs) were significantly higher in smokers than in non-smokers (Table 3). Interestingly, we found that quitting smoking changed the plasma miRNA profiles resembling those of the non-smokers (Fig. 2A). These results suggested that the differences in the plasma miRNA profiles of smokers and non-smokers were actually due to cigarette smoking. However, no association was observed between the numbers of detected miRNAs or abundance of miRNAs and plasma nicotine or cotinine levels or smoking history within smokers (data not shown). One subject who stopped smoking, S8, was a nicotine patch user. Because there was no substantial difference between the plasma miRNA profile of this subject and those of the other 3 subjects who stopped smoking, as well as those of the non-smokers, nicotine is unlikely to cause altered plasma miRNA expression. Other chemicals or oxidants in cigarette smoke, or hypoxic stress, might cause changes in plasma miRNA profiles. It would be of interest to investigate whether the miRNAs whose levels were higher in smokers than in non-smokers might be positively correlated with plasma levels of oxidative stress markers such as 8-hydroxydeoxyguanosine or malondialdehyde in smokers. It has been reported that the plasma levels of these markers were approximately 1.5 times higher in smoker than in non-smokers (Bloomer, 2007; Yamaguchi et al., 2005). Interestingly, Yamaguchi et al. (2005) reported that the levels of these oxidative stress markers were further increased within 30 min by smoking one cigarette after quitting smoking at least 10 h. The results were in contrast to our finding for miRNAs that the exposure to smoke from one cigarette did not substantially change the plasma miRNA profile. In addition, our finding is

inconsistent with a previous study reporting that urinary genotoxicity was detected 2 h after smoking one cigarette (De Flora et al., 1996). Although miR-210 and miR-373 are known to be typical miRNAs whose expression in cells was changed in response to hypoxia (Crosby et al., 2009), the levels of these miRNAs in plasma were below the cutoff values in both of smokers and non-smokers in our study. Collectively, there might be a time lag between the changes of intracellular miRNA expression and those of extracellular miRNA levels. Alternatively, consecutive and/or dynamic change of intracellular miRNA expression might be required to be reflected to the change of extracellular miRNA levels. We claim that the differences in the plasma miRNA profiles between smokers and non-smokers could be attributed to repeated smoking. An understanding of the number of cigarettes or the frequency of smoking required to cause changes in plasma miRNA profiles is left for future studies.

It is generally accepted that extracellular miRNAs mirror changes in miRNA expression in cells or tissues (Lee et al., 2012). There are some reports of the effects of cigarette smoke on miRNA expression in tissues (De Flora et al., 2012). Exposure to cigarette smoke caused down-regulation of some miRNAs in mouse and rat lungs (Izzotti et al., 2009a, 2009b), and the down-regulation in mouse lung was reversed by smoking cessation (Izzotti et al., 2011). Similar findings have been reported in humans; the levels of several miRNAs in airway epithelium (Schembri et al., 2009), placenta (Maccani et al., 2010), and alveolar macrophages (Graff et al., 2012) were lower in smokers than in non-smokers. These results led us to speculate that miRNAs in tissues, including trachea and lung, exposed to cigarette smoke might leak into blood. This might be the reason for higher levels of circulating miRNAs in smokers. Although it is not known whether extracellular miRNAs are functional, miRNAs undoubtedly function in cells; therefore, changes in miRNA expression in tissues or cells caused by exposure to cigarette smoke may have some pathophysiological significance. Integrated analysis of the expression of circulating miRNAs and the dysregulation of miRNAs and their target genes in tissues could provide insight into the initiation and progression of smoking-related diseases.

Interestingly, we noticed that 24 of the 44 miRNAs that showed a significantly different expression between smokers and non-smokers were previously reported as potential biomarkers of diseases (Table 6). Our observations show that smoking status might lead to incorrect conclusions when circulating miRNAs are used as biomarkers of diseases. Smoking status should therefore be considered when using circulating miRNAs as biomarkers of disease.

In conclusion, we found that cigarette smoking unambiguously alters plasma miRNA profiles. A larger number of miRNAs were detected and their expression levels were higher in smokers than in non-smokers. Because more than half of the miRNAs were reported to be potential biomarkers of diseases, we suggest the possibility that smoking status might complicate diagnosis. The plasma miRNA profiles that mirror changes in miRNA expression in tissues might signal smoking-related diseases. The information presented here provides new insight into an area of future research on circulating miRNAs.

Table 6
Circulating miRNAs reported to be potential biomarkers of diseases in humans.

miRNA	Disease
hsa-miR-221	Colorectal cancer↑ (Pu et al., 2010), malignant melanoma↑ (Kanemaru et al., 2011)
let-7 g	Breast cancer↑(Cookson et al., 2012)
hsa-let-7e	Papillary thyroid carcinomas↑(Yu et al., 2012)
hsa-miR-26a	Pancreatic cancer↑(Mahn et al., 2011), Type 1 diabetes↑(Nielsen et al., 2012)
hsa-miR-30c	Acute myocardial infarction↑(Meder et al., 2011)
hsa-let-7b	Acute myocardial infarction↑(Long et al., 2012b)
hsa-miR-451	Systemic lupus erythematosus↑(Wang et al., 2012a), renal cell carcinoma↓(Redova et al., 2012)
hsa-miR-27a	Type 1 diabetes↑(Nielsen et al., 2012)
hsa-miR-29a	Type 1 diabetes↑(Nielsen et al., 2012), active pulmonary tuberculosis ↑(Fu et al., 2011), colorectal cancer↑(Huang et al., 2010)
hsa-miR-191	Type 2 diabetes↓(Zampetaki et al., 2010)
hsa-miR-223	Nasopharyngeal carcinoma↑(Zeng et al., 2012), Systemic lupus erythematosus↑(Wang et al., 2012a), gastric cancer↑(Li et al., 2010) Hepatocellular carcinoma↑(Qi et al., 2011; Xu et al., 2011), Type 2 diabetes↓(Zampetaki et al., 2010), Sepsis↓(Wang et al., 2010a)
hsa-miR-328	Acute myocardial infarction↓(Wang et al., 2011)
hsa-miR-21	Breast cancer↑(Si et al., 2013), aortic stenos↑(Villar et al., in press), esophageal squamous cell carcinoma↑(Komatsu et al., 2011) Non-small cell lung cancer↑(Wei et al., 2011), gastric cancer↑(Li et al., 2010; Zheng et al., 2011-2012)
hsa-miR-106b	Gastric cancer↑(Tsujiura et al., 2010)
hsa-miR-20b	Non-small cell lung cancer↓(Silva et al., 2011)
hsa-miR-17	Nasopharyngeal carcinoma↓(Zeng et al., 2012)
hsa-miR-20a	Non-small cell lung cancer↓(Silva et al., 2011)
hsa-miR-24	Type 1 diabetes↑(Nielsen et al., 2012), Type 2 diabetes ↓(Zampetaki et al., 2010)
hsa-miR-106a	Gastric cancer↑(Tsujiura et al., 2010)
hsa-miR-126	Acute myocardial infarction↑(Long et al., 2012a), Type 2 diabetes ↓(Zampetaki et al., 2010)
hsa-miR-16	Hepatocellular carcinoma↓(Qu et al., 2011)
hsa-miR-25	Type 1 diabetes↑(Nielsen et al., 2012)
hsa-miR-195	Acute myocardial infarction↑(Long et al., 2012b), breast cancer ↑(Heneghan et al., 2010)
hsa-miR-92a	Breast cancer↓(Si et al., 2013), colorectal cancer↑(Huang et al., 2010)

Conflict of interest statement

The authors declare that there are no conflicts of interest.

Acknowledgment

This work was supported by JSPS KAKENHI Grant Number 21659030 and a grant from the Smoking Research Foundation in Japan. We are grateful to Dr. Tomokazu Konishi of Akita Prefectural University for his valuable advice and help in PCA.

References

Ambros, V., 2001. microRNAs: tiny regulators with great potential. Cell 107, 823–826.
Bloomer, R.J., 2007. Decreased blood antioxidant capacity and increased lipid peroxidation in young cigarette smokers compared to nonsmokers: impact of dietary intake. Nutr. J. 6, 39.
Bryant, R.J., Pawlowski, T., Catto, J.W., Marsden, G., Vessella, R.L., Rhees, B., Kuslich, C., Visakorpi, T., Hamdy, F.C., 2012. Changes in circulating microRNA levels associated with prostate cancer. Br. J. Cancer 106, 768–774.
Chen, X., Ba, Y., Ma, L., Cai, X., Yin, Y., Wang, K., Guo, J., Zhang, Y., Chen, J., Guo, X., Li, Q., Li, X., 2008. Characterization of microRNAs in serum: a novel class of biomarkers for diagnosis of cancer and other diseases. Cell Res. 18, 997–1006.
Cookson, V.J., Bentley, M.A., Hogan, B.V., Horgan, K., Hayward, B.E., Hazelwood, L.D., Hughes, T.A., 2012. Circulating microRNA profiles reflect the presence of breast tumours but not the profiles of microRNAs within the tumours. Cell. Oncol. 35, 301–308.
Crosby, M.E., Devlin, C.M., Glazer, P.M., Calin, G.A., Ivan, M., 2009. Emerging roles of microRNAs in the molecular responses to hypoxia. Curr. Pharm. Des. 15, 3861–3866.
De Flora, S., Camoirano, A., Bagnasco, M., Bennicelli, C., van Zandwijk, N., Wigbout, G., Qian, G.S., Zhu, Y.R., Kensler, T.W., 1996. Smokers and urinary genotoxins: implications for selection of cohorts and modulation of endpoints in chemoprevention trials. J. Cell. Biochem. 255, 92–98.
De Flora, S., Balansky, R., D'Agostini, F., Cartiglia, C., Longobardi, M., Steele, V.E., Izzotti, A., 2012. Smoke-induced microRNA and related proteome alterations. Modulation by chemopreventive agents. Int. J. Cancer 131, 2763–2773.
Duttagupta, R., Jiang, R., Gollub, J., Getts, R.C., Jones, K.W., 2011. Impact of cellular miRNAs on circulating miRNA biomarker signatures. PLoS One 6, e20769.
Fu, Y., Yi, Z., Wu, X., Li, J., Xu, F., 2011. Circulating microRNAs in patients with active pulmonary tuberculosis. J. Clin. Microbiol. 49, 4246–4251.
Graff, J.W., Powers, L.S., Dickson, A.M., Kim, J., Reisetter, A.C., Hassan, I.H., Kremens, K., Gross, T.J., Wilson, M.E., Monick, M.M., 2012. Cigarette smoking decreases global microRNA expression in human alveolar macrophages. PLoS One 7, e44066.
Hanke, M., Hoefig, K., Merz, H., Feller, A.C., Kausch, I., Jocham, D., Warnecke, J.M., Sczakiel, G., 2010. A robust methodology to study urine microRNA as tumor marker: microRNA-126 and microRNA-182 are related to urinary bladder cancer. Urol. Oncol. 28, 655–661.
He, L., Hannon, G.L., 2004. MicroRNAs: small RNAs with a big role in gene regulation. Nat. Rev. Genet. 5, 522–531.

Heneghan, H.M., Miller, N., Kelly, R., Newell, J., Kerin, M.J., 2010. Systemic miRNA-195 differentiates breast cancer from other malignancies and is a potential biomarker for detecting noninvasive and early stage disease. Oncologist 15, 673–682.
Higgins, M.W., Keller, J.B., Landis, J.R., Beaty, T.H., Burrows, B., Demets, D., Diem, J.E., Higgins, I.T., Lakatos, E., Lebowitz, M.D., 1984. Risk of chronic obstructive pulmonary disease. Collaborative assessment of the validity of the Tecumseh index of risk. Am. Rev. Respir. Dis. 130, 380–385.
Hoffmann, D., Hoffmann, I., El-Bayoumy, K., 2001. The less harmful cigarette: a controversial issue. A tribute to Ernst L. Wynder. Chem. Res. Toxicol. 14, 767–790.
Holbrook, J.H., Grundy, S.M., Hennekens, C.H., Kannel, W.B., Strong, J.P., 1984. Cigarette smoking and cardiovascular diseases. A statement for health professionals by a task force appointed by the steering committee of the American Heart Association. Circulation 70, 1114A–1117A.
Huang, Z., Huang, D., Ni, S., Peng, Z., Sheng, W., Du, X., 2010. Plasma microRNAs are promising novel biomarkers for early detection of colorectal cancer. Int. J. Cancer 127, 118–126.
Izzotti, A., Calin, G.A., Arrigo, P., Steele, V.E., Croce, C.M., De Flora, S., 2009a. Downregulation of microRNA expression in the lungs of rats exposed to cigarette smoke. FASEB J. 23, 806–812.
Izzotti, A., Calin, G.A., Steele, V.E., Croce, C.M., De Flora, S., 2009b. Relationships of microRNA expression in mouse lung with age and exposure to cigarette smoke and light. FASEB J. 23, 3243–3250.
Izzotti, A., Larghero, P., Longobardi, M., Cartiglia, C., Camoirano, A., Steele, V.E., De Flora, S., 2011. Dose-responsiveness and persistence of microRNA expression alterations induced by cigarette smoke in mouse lung. Mutat. Res. 717, 9–16.
Ji, J., Shi, J., Budhu, A., Yu, Z., Forgues, M., Roessler, S., Ambs, S., Chen, Y., Meltzer, P.S., Croce, C.M., Qin, L.X., Man, K., 2009. MicroRNA expression, survival, and response to interferon in liver cancer. N. Engl. J. Med. 361, 1437–1447.
Kanemaru, H., Fukushima, S., Yamashita, J., Honda, N., Oyama, R., Kakimoto, A., Masuguchi, S., Ishihara, T., Inoue, Y., Jinnin, M., Ihn, H., 2011. The circulating microRNA-221 level in patients with malignant melanoma as a new tumor marker. J. Dermatol. Sci. 61, 187–193.
Komatsu, S., Ichikawa, D., Takeshita, H., Tsujiura, M., Morimura, R., Nagata, H., Kosuga, T., Iitaka, D., Konishi, H., Shiozaki, A., Fujiwara, H., Okamoto, K., Otsuji, E., 2011. Circulating microRNAs in plasma of patients with oesophageal squamous cell carcinoma. Br. J. Cancer 105, 104–111.
Lee, Y., El Andaloussi, S., Wood, M.J., 2012. Exosomes and microvesicles: extracellular vesicles for genetic information transfer and gene therapy. Hum. Mol. Genet. 21, R125–R134.
Li, B.S., Zhao, Y.L., Guo, G., Li, W., Zhu, E.D., Luo, X., Mao, X.H., Zou, Q.M., Yu, P.W., Zuo, Q.F., Li, N., Tang, B., Liu, K.Y., Xiao, B., 2010. Plasma microRNAs, miR-223, miR-21 and miR-218, as novel potential biomarkers for gastric cancer detection. PLoS One 7, e41629.
Liang, Y., Ridzon, D., Wong, L., Chen, C., 2007. Characterization of microRNA expression profiles in normal human tissues. BMC Genomics 8, 166.
Long, G., Wang, F., Duan, Q., Chen, F., Yang, S., Gong, W., Wang, Y., Chen, C., Wang, D.W., 2012a. Human circulating microRNA-1 and microRNA-126 as potential novel indicators for acute myocardial infarction. Int. J. Biol. Sci. 8, 811–818.
Long, G., Wang, F., Duan, Q., Yang, S., Chen, F., Gong, W., Yang, X., Wang, Y., Chen, C., Wang, D.W., 2012b. Circulating miR-30a, miR-195 and let-7b associated with acute myocardial infarction. PLoS One 7, e50926.
Maccani, M.A., Avissar-Whiting, M., Banister, C.E., McGonnigal, B., Padbury, J.F., Marsit, C.J., 2010. Maternal cigarette smoking during pregnancy is associated with downregulation of miR-16, miR-21, and miR-146a in the placenta. Epigenetics 5, 583–589.
Mahn, R., Heukamp, L.C., Rogenhofer, S., von Ruecker, A., Müller, S.C., Ellinger, J., 2011. Circulating microRNAs (miRNA) in serum of patients with prostate cancer. Urology 77, 1265.e9–1265.e16.
Meder, B., Keller, A., Vogel, B., Haas, J., Sedaghat-Hamedani, F., Kayvanpour, E., Just, S., Borries, A., Rudloff, J., Leidinger, P., Meese, E., Katus, H.A., Rottbauer, W., 2011. MicroRNA signatures in total peripheral blood as novel biomarkers for acute myocardial infarction. Basic Res. Cardiol. 106, 13–23.
Meltzer, P.S., 2005. Cancer genomics: small RNAs with big impacts. Nature 435, 745–746.
Michael, A., Bajracharya, S.D., Yuen, P.S., Zhou, H., Star, R.A., Illei, G.G., Alevizos, I., 2010. Exosomes from human saliva as a source of microRNA biomarkers. Oral Dis. 16, 34–38.
Mitchell, P.S., Parkin, R.K., Kroh, E.M., Fritz, B.R., Wyman, S.K., Pogosova-Agadjanyan, E.L., Peterson, A., Noteboom, J., O'Briant, K.C., Allen, A., Lin, D.W., Urban, N., Drescher, C.W., Knudsen, B.S., Stirewalt, D.L., Gentleman, R., Vessella, R.L., Nelson, P.S., Martin, D.B., Tewari, M., 2008. Circulating microRNAs as stable blood-based markers for cancer detection. Proc. Natl. Acad. Sci. U. S. A. 105, 10513–10518.
Nakajima, M., Yamamoto, T., Kuroiwa, Y., Yokoi, T., 2000. Improved highly sensitive method for determination of nicotine and cotinine in human plasma by high-performance liquid chromatography. J. Chromatogr. B Biomed. Sci. Appl. 742, 211–215.
Nielsen, L.B., Wang, C., Sørensen, K., Bang-Berthelsen, C.H., Hansen, L., Andersen, M.L., Hougaard, P., Juul, A., Zhang, C.Y., Pociot, F., Mortensen, H.B., 2013. Circulating levels of microRNA from children with newly diagnosed type 1 diabetes and healthy controls: evidence that miR-25 associates to residual β-cell function and glycaemic control during disease progression. Exp. Diabetes Res (2012, Article ID 896362).
Olivieri, F., Antonicelli, R., Lorenzi, M., D'Alessandra, Y., Lazzarini, R., Santini, G., Spazzafumo, L., Lisa, R., La Sala, L., Galeazzi, R., Recchioni, R., Testa, R., Pompilio, G., Capogrossi, M.C., Procopio, A.D., 2013. Diagnostic potential of circulating miR-499-5p in elderly patients with acute non ST-elevation myocardial infarction. Int. J. Cardiol. http://dx.doi.org/10.1016/j.ijcard.2012.11.103 (in press).
Park, N.J., Zhou, H., Elashoff, D., Henson, B.S., Kastratovic, D.A., Abemayor, E., Wong, D.T., 2009. Salivary microRNA: discovery, characterization, and clinical utility for oral cancer detection. Clin. Cancer Res. 15, 5473–5477.
Pu, X.X., Huang, G.L., Guo, H.Q., Guo, C.C., Li, H., Ye, S., Ling, S., Jiang, L., Tian, Y., Lin, T.Y., 2010. Circulating miR-221 directly amplified from plasma is a potential diagnostic and prognostic marker of colorectal cancer and is correlated with p53 expression. J. Gastroenterol. Hepatol. 25, 1674–1680.
Qi, P., Cheng, S.Q., Wang, H., Li, N., Chen, Y.F., Gao, C.F., 2011. Serum microRNAs as biomarkers for hepatocellular carcinoma in Chinese patients with chronic hepatitis B virus infection. PLoS One 6, e28486.
Qu, K.Z., Zhang, K., Li, H., Afdhal, N.H., Albitar, M., 2011. Circulating microRNAs as biomarkers for hepatocellular carcinoma. J. Clin. Gastroenterol. 45, 355–360.
Redova, M., Poprach, A., Nekvindova, J., Iliev, R., Radova, L., Lakomy, R., Svoboda, M., Vyzula, R., Slaby, O., 2012. Circulating miR-378 and miR-451 in serum are potential biomarkers for renal cell carcinoma. J. Transl. Med. 10, 55.
Reid, G., Kirschner, M.B., van Zandwijk, N., 2011. Circulating microRNAs: association with disease and potential use as biomarkers. Crit. Rev. Oncol. Hematol. 80, 193–208.
Schembri, F., Sridhar, S., Perdomo, C., Gustafson, A.M., Zhang, X., Ergun, A., Lu, J., Liu, G., Zhang, X., Bowers, J., Vaziri, C., Ott, K., Sensinger, K., Collins, J.J., Brody, J.S., Getts, R., Lenburg, M.E., Spira, A., 2009. MicroRNAs as modulators of smoking-induced gene expression changes in human airway epithelium. Proc. Natl. Acad. Sci. U. S. A. 106, 2319–2324.
Shende, V.R., Goldrick, M.M., Ramani, S., Earnest, D.J., 2011. Expression and rhythmic modulation of circulating microRNAs targeting the clock gene Bmal1 in mice. PLoS One 6, e22586.
Shields, P.G., 1999. Molecular epidemiology of lung cancer. Ann. Oncol. 5, S7–S11.
Si, H., Sun, X., Chen, Y., Cao, Y., Chen, S., Wang, H., Hu, C., 2013. Circulating microRNA-92a and microRNA-21 as novel minimally invasive biomarkers for primary breast cancer. J. Cancer Res. Clin. Oncol 139, 223–229.
Silva, J., García, V., Zaballos, Á., Provencio, M., Lombardía, L., Almonacid, L., García, J.M., Domínguez, G., Peña, C., Diaz, R., Herrera, M., Varela, A., Bonilla, F., 2011. Vesicle-related microRNAs in plasma of nonsmall cell lung cancer patients and correlation with survival. Eur. Respir. J. 37, 617–623.
Tsujiura, M., Ichikawa, D., Komatsu, S., Shiozaki, A., Takeshita, H., Kosuga, T., Konishi, H., Morimura, R., Deguchi, K., Fujiwara, H., Okamoto, K., Otsuji, E., 2010. Circulating microRNAs in plasma of patients with gastric cancers. Br. J. Cancer 102, 1174–1179.
Ulrik, C.S., Lange, P., 2001. Cigarette smoking and asthma. Monaldi Arch. Chest Dis. 56, 349–353.
Vickers, K.C., Palmisano, B.T., Shoucri, B.M., Shamburek, R.D., Remaley, A.T., 2011. MicroRNAs are transported in plasma and delivered to recipient cells by high-density lipoproteins. Nat. Cell Biol. 13, 423–433.
Villar, A.V., García, R., Merino, D., Llano, M., Cobo, M., Montalvo, C., Martín-Durán, R., Hurlé, M.A., Nistal, J.F., 2013. Myocardial and circulating levels of microRNA-21 reflect left ventricular fibrosis in aortic stenosis patients. Int. J. Cardiol. http://dx.doi.org/10.1016/j.ijcard.2012.07.021 (in press).
Wang, K., Zhang, S., Marzolf, B., Troisch, P., Brightman, A., Hu, Z., Hood, L.E., Galas, D.J., 2009. Circulating microRNAs, potential biomarkers for drug-induced liver injury. Proc. Natl. Acad. Sci. U. S. A. 106, 4402–4407.
Wang, J.F., Yu, M.L., Yu, G., Bian, J.J., Deng, X.M., Wan, X.J., Zhu, K.M., 2010a. Serum miR-146a and miR-223 as potential new biomarkers for sepsis. Biochem. Biophys. Res. Commun. 394, 184–188.
Wang, K., Zhang, S., Weber, J., Baxter, D., Galas, D.J., 2010b. Export of microRNAs and microRNA-protective protein by mammalian cells. Nucleic Acids Res. 38, 7248–7259.
Wang, R., Li, N., Zhang, Y., Ran, Y., Pu, J., 2011. Circulating microRNAs are promising novel biomarkers of acute myocardial infarction. Intern. Med. 50, 1789–1795.
Wang, H., Peng, W., Ouyang, X., Li, W., Dai, Y., 2012a. Circulating microRNAs as candidate biomarkers in patients with systemic lupus erythematosus. Transl. Res. 160, 198–206.
Wang, K., Yuan, Y., Cho, J.H., McClarty, S., Baxter, D., Galas, D.J., 2012b. Comparing the microRNA spectrum between serum and plasma. PLoS One 7, e41561.
Wei, J., Gao, W., Zhu, C.J., Liu, Y.Q., Mei, Z., Cheng, T., Shu, Y.Q., 2011. Identification of plasma microRNA-21 as a biomarker for early detection and chemosensitivity of non-small cell lung cancer. Chin. J. Cancer 30, 407–414.
Xu, J., Wu, C., Che, X., Wang, L., Yu, D., Zhang, T., Huang, L., Li, H., Tan, W., Wang, C., Lin, D., 2011. Circulating microRNAs, miR-21, miR-122, and miR-223, in patients with hepatocellular carcinoma or chronic hepatitis. Mol. Carcinog. 50, 136–142.
Yamaguchi, Y., Haginaka, J., Morimoto, S., Fujijoka, Y., Kunimoto, M., 2005. Facilitated nitration and oxidation of LDL in cigarette smokers. Eur. J. Clin. Invest. 35, 186–193.
Yamanaka, H., Nakajima, M., Nishimura, K., Yoshida, R., Fukami, T., Katoh, M., Yokoi, T., 2004. Metabolic profile of nicotine in subjects whose CYP2A6 gene is deleted. Eur. J. Pharm. Sci. 22, 419–425.
Yamaura, Y., Nakajima, M., Takagi, S., Fukami, T., Tsuneyama, K., Yokoi, T., 2012. Plasma microRNA profiles in rat models of hepatocellular injury, cholestasis, and steatosis. PLoS One 7, e30250.
Yu, S., Liu, Y., Wang, J., Guo, Z., Zhang, Q., Yu, F., Zhang, Y., Huang, K., Li, Y., Song, E., Zheng, X.L., Xiao, H., 2012. Circulating microRNA profiles as potential biomarkers for diagnosis of papillary thyroid carcinoma. J. Clin. Endocrinol. Metab. 97, 2084–2092.
Zampetaki, A., Kiechl, S., Drozdov, I., Willeit, P., Mayr, U., Prokopi, M., Mayr, A., Weger, S., Oberhollenzer, F., Bonora, E., Shah, A., Willeit, J., Mayr, M., 2010. Plasma microRNA profiling reveals loss of endothelial miR-126 and other microRNAs in type 2 diabetes. Circ. Res. 107, 810–817.
Zeng, X., Xiang, J., Wu, M., Xiong, W., Tang, H., Deng, M., Li, X., Liao, Q., Su, B., Luo, Z., Zhou, Y., Zhou, M., Zeng, Z., Li, X., Shen, S., Shuai, C., Li, G., Fang, J., Peng, S., 2012. Circulating miR-17, miR-20a, miR-29c, and miR-223 combined as non-invasive biomarkers in nasopharyngeal carcinoma. PLoS One 7, e46367.
Zheng, Y., Cui, L., Sun, W., Zhou, H., Yuan, X., Huo, M., Chen, J., Lou, Y., Guo, J., 2011–2012. MicroRNA-21 is a new marker of circulating tumor cells in gastric cancer patients. Cancer Biomark. 10, 71–77.

1521-009X/41/6/1220–1230$25.00
DRUG METABOLISM AND DISPOSITION

http://dx.doi.org/10.1124/dmd.113.051714
Drug Metab Dispos 41:1220–1230, June 2013

DMD
DRUG METABOLISM AND DISPOSITION
aspet

Prilocaine- and Lidocaine-Induced Methemoglobinemia Is Caused by Human Carboxylesterase-, CYP2E1-, and CYP3A4-Mediated Metabolic Activation[S]

Ryota Higuchi, Tatsuki Fukami, Miki Nakajima, and Tsuyoshi Yokoi

Drug Metabolism and Toxicology, Faculty of Pharmaceutical Sciences, Kanazawa University, Kakuma-machi, Kanazawa, Japan

Received February 22, 2013; accepted March 25, 2013

ABSTRACT

Prilocaine and lidocaine are classified as amide-type local anesthetics for which serious adverse effects include methemoglobinemia. Although the hydrolyzed metabolites of prilocaine (*o*-toluidine) and lidocaine (2,6-xylidine) have been suspected to induce methemoglobinemia, the metabolic enzymes that are involved remain uncharacterized. In the present study, we aimed to identify the human enzymes that are responsible for prilocaine- and lidocaine-induced methemoglobinemia. Our experiments revealed that prilocaine was hydrolyzed by recombinant human carboxylesterase (CES) 1A and CES2, whereas lidocaine was hydrolyzed by only human CES1A. When the parent compounds (prilocaine and lidocaine) were incubated with human liver microsomes (HLM), methemoglobin (Met-Hb) formation was lower than when the hydrolyzed metabolites were incubated with HLM. In addition, Met-Hb formation when prilocaine and *o*-toluidine were incubated with HLM was higher than that when lidocaine and 2,6-xylidine were incubated with HLM. Incubation with diisopropyl fluorophosphate and bis-(4-nitrophenyl) phosphate, which are general inhibitors of CES, significantly decreased Met-Hb formation when prilocaine and lidocaine were incubated with HLM. An anti-CYP3A4 antibody further decreased the residual formation of Met-Hb. Met-Hb formation after the incubation of *o*-toluidine and 2,6-xylidine with HLM was only markedly decreased by incubation with an anti-CYP2E1 antibody. *o*-Toluidine and 2,6-xylidine were further metabolized by CYP2E1 to 4- and 6-hydroxy-*o*-toluidine and 4-hydroxy-2,6-xylidine, respectively, and these metabolites were shown to more efficiently induce Met-Hb formation than the parent compounds. Collectively, we found that the metabolites produced by human CES-, CYP2E1-, and CYP3A4-mediated metabolism were involved in prilocaine- and lidocaine-induced methemoglobinemia.

Introduction

Prilocaine and lidocaine are classified as amide-type local anesthetics, which prevent and relieve pain by interrupting nerve excitation and conduction via direct interaction with voltage-gated Na^+ channels to block the Na^+ current (Lipkind and Fozzard, 2005). In general, prilocaine and lidocaine are safely used in patients, although methemoglobinemia is occasionally induced (Rehman, 2001; Maimo and Redick, 2004). Methemoglobinemia is defined as a methemoglobin (Met-Hb) level >1.0% in the blood. Met-Hb is an abnormal form of hemoglobin in which iron is oxidized from the ferrous (Fe^{2+}) to the ferric state (Fe^{3+}). Because Met-Hb cannot bind and transport oxygen, increased levels of Met-Hb are associated with clinically severe symptoms (Moore et al., 2004). Met-Hb concentrations are normally maintained at roughly 1% of total hemoglobin by the action of Met-Hb reductase (Guay, 2009). Cyanosis usually occurs when Met-Hb concentrations increase above 10% and is followed by anxiety, fatigue, and tachycardia when Met-Hb levels reach 20%–50% of total hemoglobin levels. When Met-Hb levels reach 50%–70% of total hemoglobin levels, coma, and death may occur (Rodriguez et al., 1994).

When prilocaine was used for epidural analgesia and peripheral nerve block, some patients were reported to develop methemoglobinemia (Climie et al., 1967; Vasters et al., 2006). For example, when 288 mg of prilocaine was used in a 19-year-old white woman, her Met-Hb levels were observed to be 37.8% of total hemoglobin levels approximately 4 hours after injection (Kreutz and Kinni, 1983). Fetuses and infants under 6 months of age seem to be more susceptible. Lidocaine also causes methemoglobinemia, although only rarely. In fact, the number of articles that were published from 1949 through 2007 concerning lidocaine-related methemoglobinemia (12 episodes) is lower than the number of articles concerning prilocaine-related methemoglobinemia (68 episodes) (Guay, 2009). In humans, prilocaine and lidocaine are hydrolytically metabolized to the aromatic amines *o*-toluidine and 2,6-xylidine, respectively. These metabolites have been reported to cause increased levels of Met-Hb after intravenous administration to cats or rats (Onji and Tyuma, 1965; Lindstrom et al., 1969). On the basis of the results of these studies, prilocaine and lidocaine hydrolysis pathways have been suggested to play an important role in methemoglobinemia, but the metabolic enzymes that are involved in methemoglobinemia remain to be experimentally characterized. Moreover, it is unclear whether differences in methemoglobinemia frequency after prilocaine and lidocaine treatment are attributable to differences in enzymatic metabolism or differences in the potency of Met-Hb formation by their metabolites.

This work was supported in part by a Grant-in-Aid for Scientific Research from the Japan Society for the Promotion of Science [Grant 23590174].
dx.doi.org/10.1124/dmd.113.051714.
[S]This article has supplemental material available at dmd.aspetjournals.org.

ABBREVIATIONS: AADAC, arylacetamide deacetylase; BNPP, bis-(4-nitrophenyl) phosphate; CES, carboxylesterase; DFP, diisopropyl fluorophosphate; HLM, human liver microsomes; HPLC, high-performance liquid chromatography; Met-Hb, methemoglobin; NADPH-GS, NADPH-generating system; NPR, NADPH-P450 reductase; P450, cytochrome P450.

Esterases, which are expressed in human liver, plasma, and other tissues, contribute to the hydrolysis of approximately 10% of clinically therapeutic drugs, including ester, amide, and thioester bonds (Fukami and Yokoi, 2012). In particular, human carboxylesterases (CES), especially the CES1A and CES2 enzymes, are the major serine esterases that are responsible for the hydrolysis of various drugs and xenobiotics (Imai et al., 2006). Recently, we demonstrated that human arylacetamide deacetylase (AADAC) is involved in the metabolism of drugs such as flutamide, phenacetin, and rifamycins (Watanabe et al., 2009, 2010; Nakajima et al., 2011). We have more recently demonstrated that the hydrolysis of phenacetin by AADAC, which produced *p*-phenetidine, an aromatic amine metabolite, is predominantly involved in the phenacetin-induced formation of Met-Hb (Kobayashi et al., 2012). Thus, it is conceivable that CES1A, CES2, and AADAC are involved in the hydrolysis of prilocaine and lidocaine.

Ganesan et al. (2010) reported that dapsone-hydroxylamine, which is an *N*-hydroxylated metabolite of dapsone, was suspected to be a cause of dapsone-induced methemoglobinemia. The formation of dapsone-hydroxylamine is catalyzed by cytochromes P450 (P450) CYP2C19, CYP2E1, and CYP3A4. We recently reported that metabolic activation by CYP1A2 and CYP2E1 and hydrolysis of AADAC play a predominant role in phenacetin-induced methemoglobinemia (Kobayashi et al., 2012). Thus, it is conceivable that P450(s) are also involved in prilocaine- and lidocaine-induced methemoglobinemia.

On the basis of the aforementioned background studies, in the present study, we investigated the human enzymes responsible for the metabolism of prilocaine and lidocaine to clarify the mechanisms of prilocaine- and lidocaine-induced methemoglobinemia. In addition, the efficiencies of enzymatic metabolism and Met-Hb formation were compared between prilocaine and lidocaine.

Materials and Methods

Chemicals and Reagents. Lidocaine hydrochloride, 2,6-xylidine, *o*-toluidine, 4-hydroxyl-*o*-toluidine, and diisopropyl fluorophosphate (DFP) were purchased from Wako Pure Chemical Industries (Osaka, Japan). 6-Hydroxyl-*o*-toluidine and 4-hydroxyl-2,6-xylidine were purchased from Tokyo Chemical Industry (Tokyo, Japan). Prilocaine hydrochloride and bis-(4-nitrophenyl)-phosphate (BNPP) were obtained from Sigma-Aldrich (St. Louis, MO). Human liver microsomes (HLM; pooled, n = 50); recombinant human CYP1A2, CYP2A6, CYP2C8, CYP2D6 [with NADPH-P450 reductase (NPR)], CYP2B6, CYP2C9, CYP2C19, CYP2E1, and CYP3A4 (with NPR and cytochrome b_5) enzymes expressed in baculovirus-infected insect cells; monoclonal mouse anti-human CYP1A2 antibody; anti-human CYP2E1 antibody; and anti-human CYP3A4 antibody were purchased from BD Gentest (Woburn, MA). Other chemicals were of the highest commercially available grade.

Mouse and Human Red Blood Cells. Animals were maintained in accordance with the National Institutes of Health Guide for Animal Welfare of Japan, and the protocols were approved by the Institutional Animal Care and Use Committee of Kanazawa University, Japan. The use of human red blood cells was approved by the Ethics Committees of Kanazawa University (Kanazawa, Japan). Mouse blood (pooled samples from 5 C57BL/6J mice: 6-week-old male, 20–25 g) that had been obtained from SLC Japan (Hamamatsu, Japan) and human blood samples (from five healthy Japanese volunteers: 22–30-year-old males) were obtained according to our previous report (Kobayashi et al., 2012). All assays were performed immediately after the separation of the red blood cells.

Prilocaine and Lidocaine Hydrolase Activities. Prilocaine and lidocaine hydrolase activities were determined as follows: a typical incubation mixture (final volume of 0.2 ml) contained 100 mM potassium phosphate buffer (pH 7.4) and various enzyme sources (HLM or Sf21 cell homogenates expressing esterases, 0.4 mg/ml). Sf21 cell homogenates expressing CES1A, CES2, or AADAC were prepared as previously described (Fukami et al., 2010; Watanabe et al., 2010). In a preliminary study, we confirmed that the formation rates of *o*-toluidine and 2,6-xylidine from prilocaine and lidocaine, respectively, were linear with respect to protein concentration (< 2.0 mg/ml) and incubation time (<120 minutes). Prilocaine and lidocaine were dissolved in distilled water. The reactions were initiated by the addition of prilocaine and lidocaine (0.2–10 mM for HLM or 0.1–4 mM for Sf21 cell homogenates expressing esterases) after a 2-minute preincubation at 37°C. After a 30-minute incubation, the reactions were terminated by the addition of 10 μl of ice-cold 60% perchloric acid. After removal of the protein by centrifugation at 9500*g* for 5 minutes, a 60-μl portion of the supernatant was subjected to high-performance liquid chromatography (HPLC). The HPLC analysis was performed using an L-7100 pump (Hitachi, Tokyo, Japan), an L-7200 autosampler (Hitachi), an L-7405 UV detector (Hitachi), and a D-2500 Chromato-Integrator (Hitachi) equipped with a Wakopak eco-ODS column (5-μm particle size, 4.6 mm i.d.×150 mm; Wako Pure Chemical Industries). The eluent was monitored at 210 nm with a noise-base clean Uni-3 (Union, Gunma, Japan), which can reduce the noise by integrating the output and increase the signal by 3-fold by differentiating the output and by 5-fold by further amplification with an internal amplifier, resulting in a maximum 15-fold amplification of the signal. The mobile phase was 35% methanol containing 0.2% phosphoric acid and 2.2 mM sodium 1-octanesulfonate. The flow rate was 1.0 ml/min. The column temperature was 35°C. The quantification of *o*-toluidine and 2,6-xylidine was performed by comparing the HPLC peak height with that of an authentic standard. The limit of quantification in the reaction mixture for *o*-toluidine and 2,6-xylidine was 100 nM, with a coefficient of variation <5.6%. The activity at each concentration was determined as the mean value in triplicate. For kinetic analyses of the prilocaine and lidocaine hydrolase activities, the parameters were estimated from the fitted curves with use of a computer program (KaleidaGraph; Synergy Software, Reading, PA) that was designed for use in nonlinear regression analyses.

Met-Hb Formation. A Met-Hb formation assay was conducted according to the methods outlined in our previous study (Kobayashi et al., 2012), with a slight modification. A typical incubation mixture (final volume of 0.2 ml) contained 5% of the mouse red blood cell fraction except in (7), where human red blood cell fraction was used, 100 mM potassium phosphate buffer (pH 7.4), an NADPH-generating system (NADPH-GS: 0.5 mM $NADP^+$, 5 mM glucose 6-phosphate, 5 mM $MgCl_2$, and 1 U/ml glucose-6-phosphate dehydrogenase), and various enzyme sources.

1. To investigate the time-dependence of Met-Hb formation, HLM (1.0 mg/ml) were used as enzyme sources. The reactions were initiated by the addition of prilocaine, lidocaine, *o*-toluidine, or 2,6-xylidine (1 mM) after a 2-minute preincubation at 37°C. After the 0–120-minute incubation at 37°C, the reaction was terminated by placing the samples on ice.
2. To investigate the concentration-dependence of Met-Hb formation, HLM (1.0 mg/ml) were used as enzyme sources. The reactions were initiated by the addition of prilocaine, lidocaine, *o*-toluidine, or 2,6-xylidine (0.01, 0.1, 1, or 10 mM) after a 2-minute preincubation at 37°C. After the 60-minute incubation at 37°C, the reaction was terminated by placing the samples on ice.
3. To determine the P450 enzymes that were involved in prilocaine-, lidocaine-, *o*-toluidine-, and 2,6-xylidine–induced Met-Hb formation, recombinant human P450 enzymes (25 pmol /ml) were used as enzyme sources. The reactions were initiated by the addition of prilocaine (10 mM), lidocaine (10 mM), *o*-toluidine (1 mM), or 2,6-xylidine (1 mM) after a 2-minute preincubation at 37°C. After the 120-minute incubations (prilocaine and lidocaine) and the 60-minute incubations (*o*-toluidine and 2,6-xylidine) at 37°C, the reactions were terminated by placing the samples on ice.
4. To investigate the involvement of various esterase(s) in the HLM, inhibition analyses of prilocaine- and lidocaine-induced Met-Hb formation were performed using the general CES inhibitors DFP and BNPP (Watanabe et al., 2009). HLM (1.0 mg/ml) were used as enzyme sources, and the concentrations of inhibitors were 100 μM. DFP and BNPP were dissolved in distilled water. The reaction conditions were the same as those described in (3).
5. To investigate the involvement of P450 enzymes in the HLM in Met-Hb formation, inhibition analyses of the formation of Met-Hb by prilocaine

(10 mM), lidocaine (10 mM), *o*-toluidine (1 mM), or 2,6-xylidine (1 mM) were performed using anti-P450 antibodies. HLM (0.5 mg/ml) were used as enzyme sources. Ten microliters of antibody-mixtures [4 μl of anti-CYP2E1 antibody mixed with 6 μl of 25 mM Tris-buffer (pH 7.5) or 10 μl of anti-CYP1A2 or anti-CYP3A4 antibody] was incubated on ice for 30 minutes with enzyme sources, after which typical incubation mixtures (final volume of 0.2 ml) that included the antibody mixtures were prepared. To investigate the involvement of P450 enzymes in prilocaine- and lidocaine-induced Met-Hb formation in the absence of a hydrolysis reaction, DFP (100 μM) was added into the incubation mixture. The reaction conditions were the same as those described in (3).

6. To investigate whether the hydroxylated metabolites of *o*-toluidine and 2,6-xylidine induced Met-Hb formation, *o*-toluidine, 4-hydroxy-*o*-toluidine, 6-hydroxy-*o*-toluidine, 2,6-xylidine, and 4-hydroxy-2,6-xylidine (1 mM) were incubated with HLM (1.0 mg/ml) and mouse red blood cells both in the presence and absence of an NADPH-GS. After a 60-minute incubation at 37°C, the reactions were terminated by placing the samples on ice.
7. To investigate the sensitivity of human red blood cells to prilocaine- and lidocaine-induced Met-Hb formation, a Met-Hb formation assay was conducted using human red blood cells instead of mouse red blood cells. HLM (1.0 mg/ml) were used as enzyme sources, and DFP (100 μM) was added into the incubation mixture. The reaction was initiated by the addition of 10 mM prilocaine and lidocaine after a 2-minute preincubation at 37°C. The reaction conditions were the same as those described in (3).

Prilocaine and lidocaine were dissolved in distilled water. *o*-Toluidine and 2,6-xylidine were dissolved in acetonitrile, and the final concentration of acetonitrile in the incubation mixture was 1%. It has been reported that 1% acetonitrile does not inhibit the activities of CYP1A2, CYP2E1, and CYP3A4 (Chauret et al., 1998).

The Met-Hb levels in red blood cells were determined as the percentage of total hemoglobin according to the methods outlined in our previous study (Kobayashi et al., 2012)

Normalizing Met-Hb Formation by P450 Levels in HLM. Met-Hb formation was normalized by the levels of each P450 enzyme in HLM and was calculated using the following equation, where the $P450_{HLM}$ activity and $P450_{expression}$ activity values are the marker activities of each P450 in HLM and recombinant P450 expression systems, respectively:

$$\text{Met-Hb formation normalized by P450 levels in HLM (\%)} = \text{Met-Hb formation by recombinant human P450 expression systems (\%)} \times P450_{HLM}\ \text{activity}/P450_{expression}$$

The reaction conditions for Met-Hb formation by recombinant human P450 expression systems were determined as follows: prilocaine, lidocaine (10 mM), and their hydrolyzed metabolites (1 mM) were incubated with each P450 expression system (25 pmol P450/ml), an NADPH-GS, and mouse red blood cells. The incubation time was either 120 minutes (prilocaine and lidocaine) or 60 minutes (*o*-toluidine and 2,6-xylidine).

The reaction conditions for Met-Hb formation in HLM were determined as described in the above paragraph, except HLM (1.0 mg/ml) were used in place of the P450 expression systems. Met-Hb formation was detected as described in (3) above.

Methoxyresorufin *O*-demethylase, chlorzoxazone 6-hydroxylase, and midazolam 1′-hydroxylase activities were measured as markers for the activities of CYP1A2, CYP2E1, and CYP3A4, respectively, by HPLC, according to methods described in our previous reports (Nakajima et al., 2002; Fukami et al., 2007, 2008).

***o*-Toluidine and 2,6-Xylidine Hydroxylase Activities.** The activities of *o*-toluidine and 2,6-xylidine hydroxylase were determined as follows: a typical incubation mixture (final volume of 0.2 ml) contained *o*-toluidine or 2,6-xylidine (4–200 μM), 100 mM potassium phosphate buffer (pH 7.4), an NADPH-GS, and HLM (0.4 mg/ml). In a preliminary study, we confirmed that the formation rates of 4-hydroxyl-*o*-toluidine and 6-hydroxyl-*o*-toluidine from *o*-toluidine, as well as 4-hydroxyl-2,6-xylidine from 2,6-xylidine, in HLM were linear with respect to protein concentration (< 1.0 mg/ml) and incubation time (<60 minutes). *o*-Toluidine and 2,6-xylidine were dissolved in acetonitrile, and the final concentration of acetonitrile in the incubation mixture was 1%.

Inhibition analyses of *o*-toluidine or 2,6-xylidine hydroxylation were performed using anti-P450 antibodies. HLM (0.4 mg/ml) were used as enzyme sources. Eight microliters of antibody-mixtures [3.2 μl of anti-CYP2E1 antibody mixed with 4.8 μl of 25 mM Tris-buffer (pH 7.5) or 8 μl of anti-CYP1A2 or anti-CYP3A4 antibody] was incubated with enzyme sources on ice for 30 minutes. Then, typical incubation mixtures (final volume of 0.2 ml) were prepared by the addition of *o*-toluidine (50 μM) or 2,6-xylidine (30 μM).

The reactions were initiated by the addition of an NADPH-GS after a 2-minute preincubation at 37°C. After a 30-minute incubation, the reactions were terminated by the addition of 10 μl of ice-cold 60% perchloric acid. After removal of the protein by centrifugation at 9500*g* for 5 minutes, a 50-μl portion of the supernatant was subjected to HPLC. The HPLC equipment was the same as that described above. The mobile phase for *o*-toluidine hydroxylation was 8.5% methanol/8% acetonitrile containing 0.2% phosphoric acid and 2.2 mM sodium 1-octanesulfonate, and the mobile phase for 2,6-xylidine hydroxylation was 10% acetonitrile containing 0.11% phosphoric acid and 2.2 mM sodium 1-octanesulfonate. The quantification of the hydroxylated metabolites of *o*-toluidine and 2,6-xylidine was performed by comparing the HPLC peak height with that of an authentic standard. The activity at each concentration was determined as the mean value in triplicate. For kinetic analyses of the *o*-toluidine and 2,6-xylidine hydroxylase activities, the parameters were estimated as described above.

Statistical Methods. Statistical analyses between two and multiple groups were performed using an unpaired, two-tailed Student's *t* test and analysis of variance, followed by Tukey's post-hoc test. $P < 0.05$ was considered to be statistically significant.

Results

Prilocaine and Lidocaine Hydrolase Activities in HLM. Because hydrolysis of prilocaine and lidocaine was suspected to play an important role in methemoglobinemia, we investigated whether microsomes of the human liver, which is the main organ for drug metabolism and expresses various esterases, could hydrolyze prilocaine and lidocaine (Fig. 1, A and B). Data for these hydrolase activities in HLM followed Michaelis-Menten kinetics. The K_m and V_{max} values for the hydrolysis of prilocaine in HLM were 1.15 ± 0.01 mM and 2.46 ± 0.04 nmol/min/mg protein, respectively, resulting in a CL_{int} value of 2.14 ± 0.04 μl/min/mg protein. The K_m and V_{max} values for the hydrolysis of lidocaine in HLM were 0.96 ± 0.06 mM and 0.62 ± 0.01 nmol/min/mg protein, respectively, resulting in a CL_{int} value of 0.66 ± 0.03 μl/min/mg protein (Table 1). Thus, the CL_{int} value for the hydrolysis of prilocaine was shown to be 3.2 higher than that of lidocaine. These results indicated that HLM have a higher metabolic efficiency for prilocaine hydrolysis than for lidocaine hydrolysis.

Prilocaine and Lidocaine Hydrolase Activities by Recombinant Human CES1A and CES2. To confirm that human CES1A, CES2, and AADAC, which are typical serine esterases that are involved in the hydrolysis of numerous drugs, can hydrolyze prilocaine and lidocaine, prilocaine and lidocaine hydrolase activities were measured using recombinant human CES1A, CES2, and AADAC expressed in Sf21 cells (Fig. 1, C and D). Data for these hydrolase activities followed Michaelis-Menten kinetics. The K_m and V_{max} values for prilocaine hydrolase activity by CES1A were 0.31 ± 0.01 mM and 0.40 ± 0.01 nmol/min/mg protein, respectively, resulting in a CL_{int} value of 1.29 ± 0.04 μl/min/mg protein (Table 1). CES2 displayed the prilocaine hydrolase activity with K_m, V_{max}, and CL_{int} values of 0.39 ± 0.01 mM, 0.10 ± 0.00 nmol/min/mg protein, and 0.26 ± 0.00 μl/min/mg protein, respectively. The K_m, V_{max}, and CL_{int} values for lidocaine hydrolysis by CES1A were 0.35 ± 0.06 mM, 0.14 ± 0.00 nmol/min/mg protein, and 0.40 ± 0.02 μl/min/mg

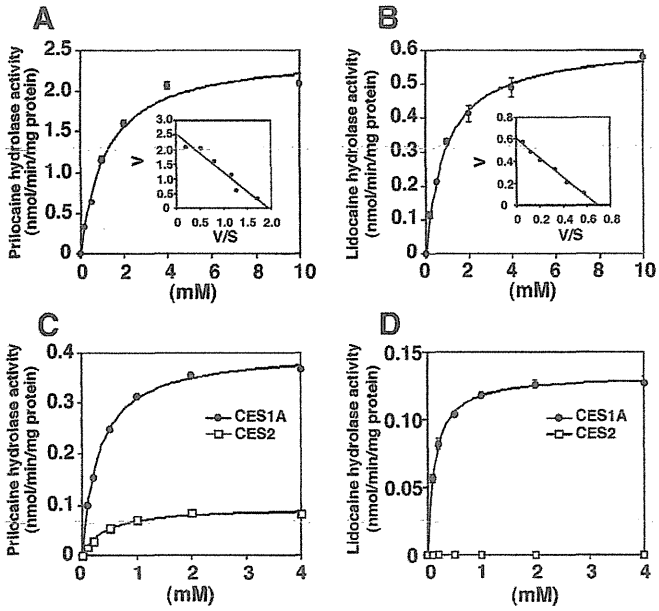

Fig. 1. Kinetic analyses of prilocaine and lidocaine hydrolase activities in HLM and recombinant human CES1A and CES2 expressed in Sf21 cells. HLM (0.4 mg/ml) (A and B) or CES1A and CES2 (0.2 mg/ml) (C and D) were incubated with prilocaine (A and C) and lidocaine (B and D) for 30 minutes. Hydrolase activities for prilocaine and lidocaine were measured by quantitative analyses of *o*-toluidine and 2,6-xylidine, respectively, using HPLC. Each data point represents the mean ± S.D. of triplicate determinations.

protein, respectively, whereas CES2 did not display any lidocaine hydrolase activity (Table 1). AADAC did not display hydrolase activities for either prilocaine or lidocaine. These results indicate that the metabolic efficiency of prilocaine hydrolysis by CES1A was higher than that of lidocaine hydrolysis. CES2 participated in prilocaine hydrolysis but not lidocaine hydrolysis.

Formation of Met-Hb by Prilocaine or Lidocaine and Their Metabolites. To investigate Met-Hb formation in vitro, prilocaine, lidocaine, or their hydrolyzed metabolites, *o*-toluidine and 2,6-xylidine, were incubated with HLM, an NADPH-GS, and mouse red blood cells for 0–120 minutes. Met-Hb formation was linear with respect to incubation time (1 mM prilocaine or lidocaine <120 minutes, 1 mM *o*-toluidine or 2,6-xylidine <60 minutes) (Fig. 2A).

To compare the induction potency of Met-Hb formation among prilocaine, lidocaine, *o*-toluidine, and 2,6-xylidine, the compounds were incubated at various concentrations (Fig. 2B). Met-Hb formation increased in a concentration-dependent manner. *o*-Toluidine and 2,6-xylidine more efficiently induced Met-Hb formation, compared

TABLE 1

Kinetic parameters of the hydrolase activities of prilocaine and lidocaine

Data are the mean ± S.D. of triplicate determinations.

Drug	Enzyme Source	K_m	V_{max}	CL_{int}
		mM	*nmol/min/mg protein*	*μl/min/mg protein*
Prilocaine	HLM	1.15 ± 0.01	2.46 ± 0.04	2.14 ± 0.04
	CES1A	0.31 ± 0.01	0.40 ± 0.01	1.29 ± 0.04
	CES2	0.39 ± 0.01	0.10 ± 0.00	0.26 ± 0.00
	AADAC	ND	ND	—
Lidocaine	HLM	0.96 ± 0.06	0.62 ± 0.01	0.66 ± 0.03
	CES1A	0.35 ± 0.06	0.14 ± 0.00	0.40 ± 0.02
	CES2	ND	ND	—
	AADAC	ND	ND	—

ND, not detected.

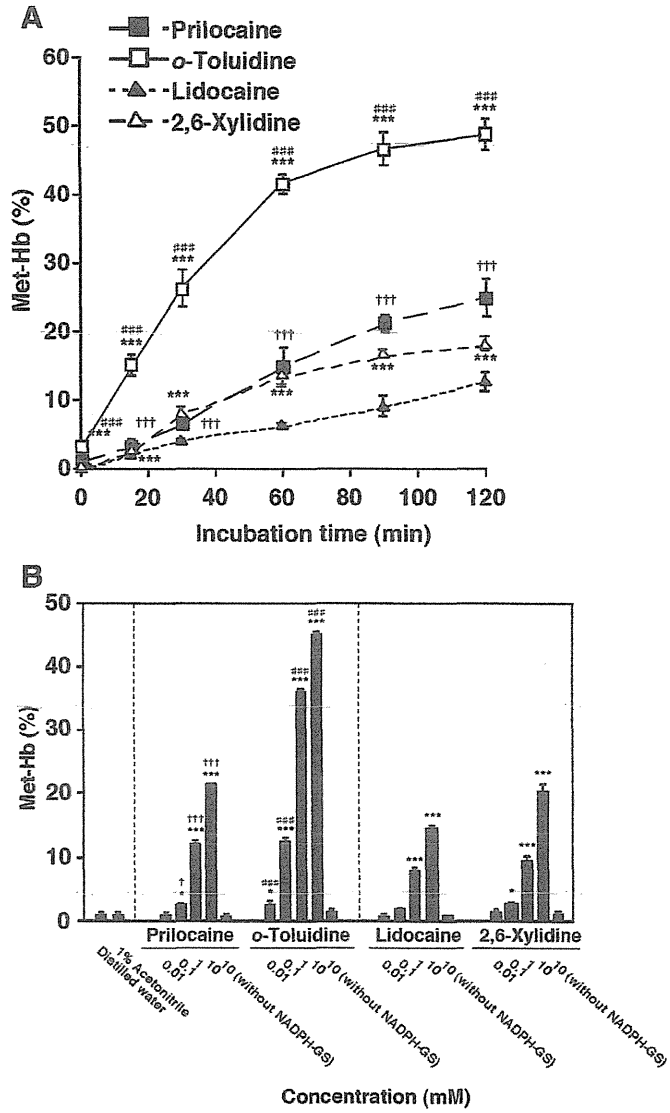

Fig. 2. (A) Time-dependent prilocaine-, lidocaine-, *o*-toluidine–, and 2,6-xylidine–induced Met-Hb formation. Prilocaine, lidocaine, and their hydrolyzed metabolites (1 mM) were incubated for 0–120 minutes with HLM (1.0 mg/ml), an NADPH-GS, and mouse red blood cells. Each data point represents the mean ± S.D. of triplicate determinations. Differences in Met-Hb formation, compared with the corresponding parent compounds at the same incubation time, were considered to be significant at $^{***}P < 0.001$. Differences in prilocaine- and lidocaine-induced Met-Hb formation at the same incubation time were considered to be significant at $^{\dagger\dagger\dagger}P < 0.001$. Differences in *o*-toluidine– and 2,6-xylidine–induced Met-Hb formation at the same incubation time were considered to be significant at $^{\#\#\#}P < 0.001$. (B) Concentration-dependent prilocaine-, lidocaine-, *o*-toluidine–, and 2,6-xylidine–induced Met-Hb formation. Prilocaine, lidocaine, and their hydrolyzed metabolites (0.01–10 mM) were incubated with HLM (1.0 mg/ml), an NADPH-GS, and mouse red blood cells for 60 minutes. Each column represents the mean ± S.D. of triplicate determinations. Differences in Met-Hb formation, compared with the corresponding vehicle-treated controls, were considered to be significant at $^{*}P < 0.05$; $^{***}P < 0.001$. Differences in prilocaine- and lidocaine-induced Met-Hb formation at the same concentration were considered to be significant at $^{\dagger}P < 0.05$; $^{\dagger\dagger\dagger}P < 0.001$. Differences in *o*-toluidine– and 2,6-xylidine–induced Met-Hb formation at the same concentration were considered to be significant at $^{\#\#\#}P < 0.001$.

with their corresponding parent drugs. This result suggested that the hydrolyzed metabolites enhanced prilocaine- or lidocaine-induced Met-Hb formation. Prilocaine-induced Met-Hb formation was significantly higher than lidocaine-induced formation at each concentration that was greater than 0.1 mM. In the same manner, *o*-toluidine–induced Met-Hb formation was significantly higher than 2,6-xylidine–induced

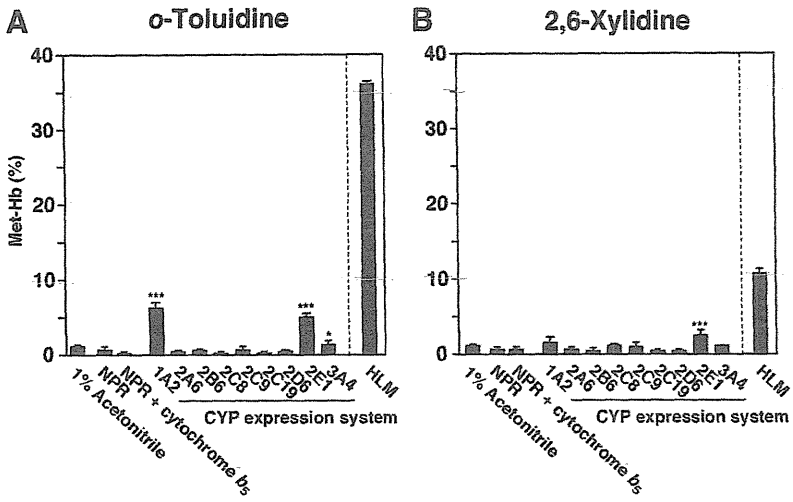

Fig. 3. The effects of P450 (CYP) enzymes on *o*-toluidine– and 2,6-xylidine–induced Met-Hb formation. Each individual recombinant human P450 expression system (25 pmol P450/ml) or HLM (1.0 mg/ml) was incubated with 1 mM *o*-toluidine (A) or 2,6-xylidine (B), an NADPH-GS, and mouse red blood cells for 60 minutes. Each column represents the mean ± S.D. of triplicate determinations. Differences in Met-Hb formation, compared with NPR or NPR + cytochrome b_5 (control supersomes expressing no P450s), were considered to be significant at $^*P < 0.05$; $^{***}P < 0.001$.

formation at each concentration that was greater than 0.1 mM. The increased Met-Hb formation that was induced by prilocaine, lidocaine, and their hydrolyzed metabolites was not observed in the absence of an NADPH-GS (Fig. 2B). These results suggest that the potency of prilocaine to induce Met-Hb formation was approximately 1.5-fold higher than that of lidocaine at the same concentration and that the NADPH-dependent enzymes that are expressed in HLM are essential for Met-Hb formation.

Met-Hb Formation after the Metabolic Activation of *o*-Toluidine and 2,6-Xylidine by Human P450(s). As outlined above, NADPH-dependent enzyme(s) are essential for prilocaine- and lidocaine-induced Met-Hb formation. Therefore, the involvement of representative NADPH-dependent enzymes (the P450 enzymes) in *o*-toluidine and 2,6-xylidine metabolism was investigated (Fig. 3). Either *o*-toluidine or 2,6-xylidine (1 mM) was incubated with recombinant human P450s, an NADPH-GS, and mouse red blood cells. *o*-Toluidine–induced Met-Hb formation was significantly increased by CYP1A2 (6.2% ± 0.7%), CYP2E1 (5.0% ± 0.4%), and CYP3A4 (1.3% ± 0.5%), and 2,6-xylidine–induced Met-Hb formation was increased by CYP2E1 (2.3% ± 0.8%).

Prilocaine- and Lidocaine-Induced Met-Hb Formation Inhibition Analyses in the Presence of Esterase Inhibitors. To investigate the involvement of human CES in prilocaine- and lidocaine-induced methemoglobinemia, inhibition analyses were performed with DFP and BNPP, which are potent CES inhibitors (Watanabe et al., 2009) (Fig. 4). The hydrolase activities of prilocaine and lidocaine (1 mM) in HLM (1.0 mg/ml) were preliminarily confirmed by HPLC to be completely inhibited by 10 μM DFP and 10 μM BNPP (unpublished data). When prilocaine and lidocaine (10 mM) were incubated with HLM, an NADPH-GS, and mouse red blood cells in the presence of DFP or BNPP (100 μM), both prilocaine- and lidocaine-induced Met-Hb formation were decreased (prilocaine, percentage of control: 31.6% in the presence of DFP and 34.0% in the presence of BNPP; lidocaine, percentage of control: 56.6% in the presence of DFP and 56.6% in the presence of BNPP) (Fig. 4). DFP and BNPP did not alter Met-Hb formation (unpublished data). Thus, CES were determined to be involved in Met-Hb formation.

Met-Hb Formation after the Metabolic Activation of Prilocaine and Lidocaine by Human P450(s). As shown in Fig. 4, DFP and BNPP could not completely inhibit prilocaine- and lidocaine-induced Met-Hb formation, suggesting that the metabolic activation of prilocaine and lidocaine by P450 enzyme(s) may mediate Met-Hb formation in the absence of hydrolysis. When prilocaine and lidocaine (10 mM) were incubated with representative recombinant human P450s, an NADPH-GS, and mouse red blood cells, Met-Hb formation increased in the presence of CYP3A4 (1.7% ± 0.2% for prilocaine and 1.1% ± 0.4% for lidocaine) (Fig. 5). These results suggest that prilocaine- and lidocaine-induced Met-Hb formation in the absence of hydrolysis is catalyzed by metabolic activation by human CYP3A4.

Normalizing Met-Hb Formation by P450 Levels in HLM. Because each P450 enzyme is expressed at different levels in HLM, we were unable to simply compare the contribution of each P450 enzyme to prilocaine-, lidocaine-, *o*-toluidine–, or 2,6-xylidine–induced Met-Hb formation in HLM with use of human P450 expression systems. Therefore, to estimate the contributions of P450 enzymes in HLM, Met-Hb formation in the presence of recombinant P450 expression systems was normalized by the levels of each P450 enzyme in HLM (Fig. 6). For *o*-toluidine– and 2,6-xylidine–induced Met-Hb formation, CYP2E1 had the highest contribution in HLM,

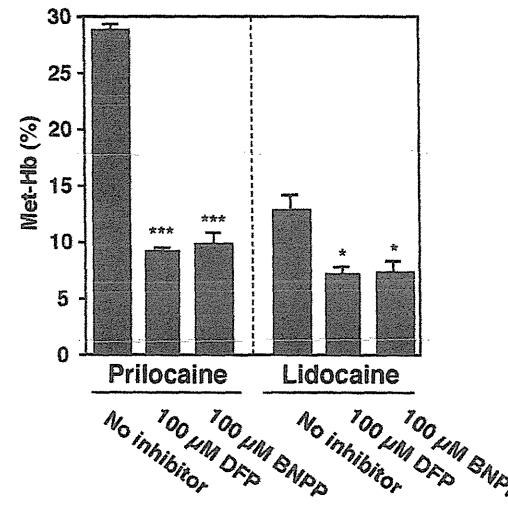

Fig. 4. The effects of DFP or BNPP on prilocaine- and lidocaine-induced Met-Hb formations. HLM (1.0 mg/ml) were incubated with prilocaine or lidocaine (10 mM), an NADPH-GS, and mouse red blood cells for 120 minutes. The concentration of DFP or BNPP was 100 μM. Each column represents the mean ± S.D. of triplicate determinations. Prilocaine- and lidocaine-induced Met-Hb formation in the absence of inhibitors was 28.8% ± 0.5% and 12.9% ± 1.3%, respectively. Differences compared with the controls lacking inhibitor were considered to be significant at $^*P < 0.05$; $^{***}P < 0.001$.

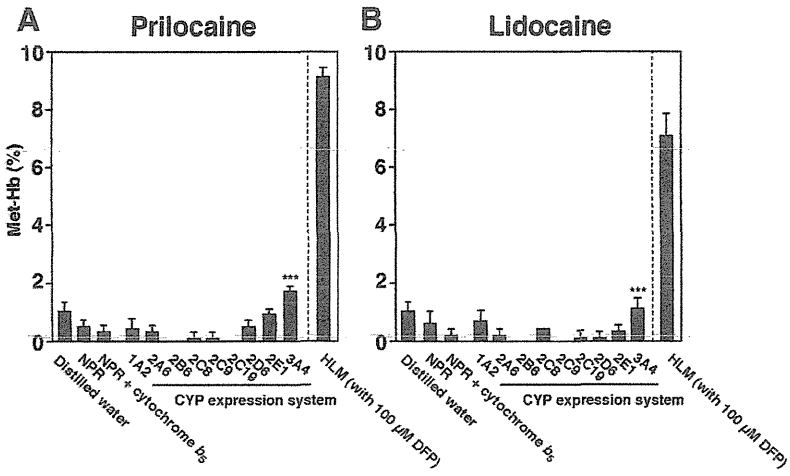

Fig. 5. The effects of P450 (CYP) enzymes on prilocaine- and lidocaine-induced Met-Hb formation without hydrolysis pathway. Each individual recombinant human P450 expression system (25 pmol P450/ml) or HLM (1.0 mg/ml) was incubated with 10 mM prilocaine (A) or lidocaine (B), an NADPH-GS, and mouse red blood cells for 120 minutes. Each column represents the mean ± S.D. of triplicate determinations. Differences in Met-Hb formation, compared with NPR or NPR + cytochrome b_5 (control supersomes expressing no P450s), were considered to be significant at $^*P < 0.05$; $^{***}P < 0.001$.

whereas CYP1A2 and CYP3A4 had relatively low contributions (Fig. 6, A and B). For prilocaine- and lidocaine-induced Met-Hb formation, CYP3A4 had the highest contribution in HLM (Fig. 6, C and D). Although flavin-containing monooxygenase is also known to be an NADPH-dependent enzyme, Met-Hb formation that was induced by prilocaine, lidocaine, and their hydrolyzed metabolites in HLM was not inhibited by 1 mM methimazole, which is a competitive flavin-containing monooxygenase inhibitor (unpublished data) (Rawden et al., 2000). Thus, CYP2E1 was determined to contribute highly to *o*-toluidine– and 2,6-xylidine–induced Met-Hb formation, whereas CYP3A4 was determined to contribute highly to prilocaine- and lidocaine-induced Met-Hb formation.

Met-Hb Formation Inhibition Analyses after the Incubation of Prilocaine, Lidocaine, and Their Hydrolyzed Metabolites with Anti-P450 Antibodies. To further investigate the contributions of CYP1A2, CYP2E1, and CYP3A4 to the *o*-toluidine– and 2,6-xylidine–induced Met-Hb formation in HLM, inhibition analyses were performed using anti-P450 antibodies (Fig. 7A). *o*-Toluidine– and 2,6-xylidine–induced Met-Hb formation were markedly decreased by incubation with an anti-CYP2E1 antibody (from 19.5% ± 0.6% to 7.1% ± 0.4% for

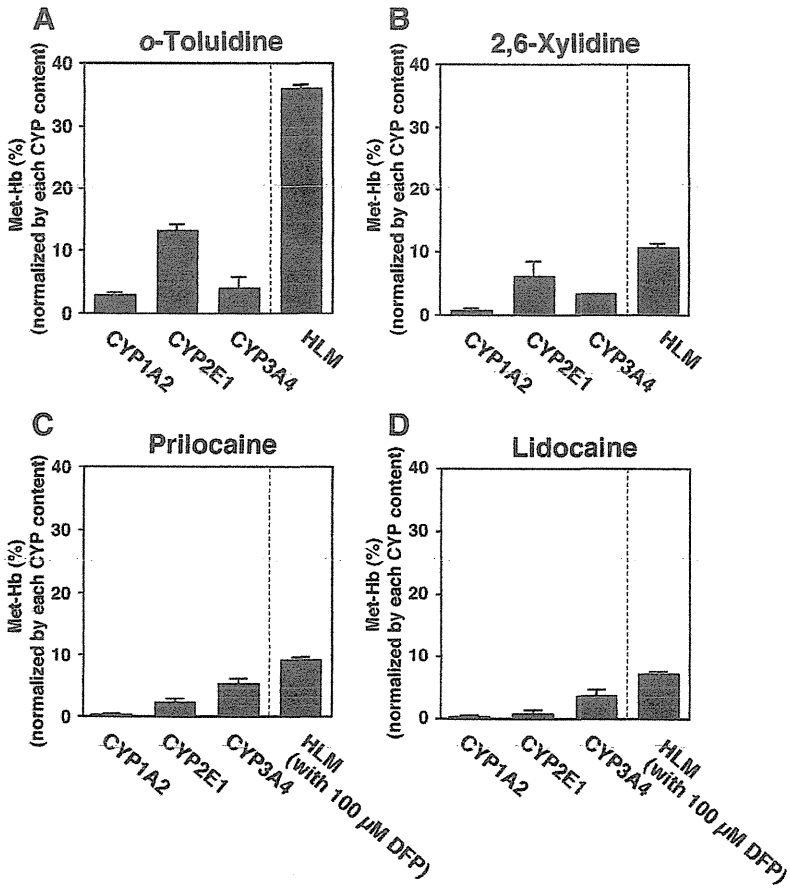

Fig. 6. Met-Hb formation normalized by the levels of each P450 (CYP) in HLM. Met-Hb formation was normalized by the levels of each P450 and calculated according to the equation described in *Materials and Methods*. Prilocaine, lidocaine (10 mM) (A and C), and their hydrolyzed metabolites (1 mM) (B and D) were incubated with each P450 expression system (25 pmol P450/ml), an NADPH-GS, and mouse red blood cells. The incubation time was 120 minutes (prilocaine and lidocaine) or 60 minutes (*o*-toluidine and 2,6-xylidine). Each column represents the mean ± S.D. of triplicate determinations.